ORGANOMETALLICS

Article

pubs.acs.org/Organometallics

Insights into the Stability and Structures of Phosphine-Boranes and Their α-Metalated Derivatives

Keith Izod,* Corinne Wills,* Emma Anderson, Ross W. Harrington, and Michael R. Probert

Main Group Chemistry Laboratories, School of Chemistry, Newcastle University, Bedson Building, Newcastle upon Tyne, NE1 7RU, U.K.

Supporting Information

ABSTRACT: The reaction between iPr$_2$PCl and Ph$_2$P(BH$_3$)CH$_2$Li gives the mixed phosphine/phosphine-borane Ph$_2$P(BH$_3$)CH$_2$PiPr$_2$ (**1a**) in good yield. Thermolysis of **1a** leads to borane migration and the formation of Ph$_2$PCH$_2$P(BH$_3$)iPr$_2$ (**2a**) along with small amounts of Ph$_2$P(BH$_3$)CH$_2$P(BH$_3$)iPr$_2$ (**3a**) and Ph$_2$PCH$_2$PiPr$_2$ (**4a**). Compound **3a** may be synthesized directly from the reaction of **1a** with BH$_3$·SMe$_2$, while **4a** can be prepared cleanly by heating **1a** in methanol under reflux. Kinetic studies on the conversion of **1a** to **2a** reveal the reaction to be apparently first order in **1a**, suggesting a dissociative process, and yield the activation parameters $\Delta H^{\ddagger} = 63 \pm 8$ kJ mol^{-1}, $\Delta S^{\ddagger} = -145 \pm 24$ J K^{-1} mol^{-1}, and $\Delta G^{\ddagger} = 106 \pm 8$ kJ mol^{-1}, the negative entropy of activation conversely suggesting an associative process. DFT studies suggest that concerted migration of borane within a molecule of **1a** is disfavored, but that both the dissociative and associative mechanisms for borane migration operate simultaneously. Metalation of **1a**−**4a** with nBuLi in the presence of tmeda gives the complexes [{Ph$_2$P(BH$_3$)}CHPiPr$_2$]Li(tmeda) (**1b**), [Ph$_2$PCH{P(BH$_3$)iPr$_2$}]Li(tmeda) (**2b**), [{Ph$_2$P(BH$_3$)}CH{P(BH$_3$)iPr$_2$}]Li(tmeda) (**3b**), and [Ph$_2$PCHPiPr$_2$]Li(tmeda) (**4b**), respectively, which adopt similar structures in the solid state. Analysis of the crystal structures suggests that the phosphine-borane groups stabilize the adjacent charge to a greater extent than the phosphine groups. This is supported by DFT calculations, which show that the greatest delocalization of negative charge from the carbanion is into the P−C(Ph) or P−C(Pr) σ*-orbitals of the phosphine-borane substituents.

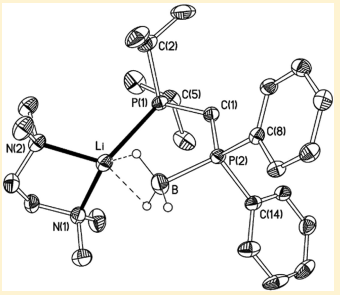

INTRODUCTION

Phosphine-borane adducts, R$_3$P-BH$_3$, rank among the most useful precursor materials in organophosphorus chemistry and are key intermediates in the synthesis of a wide array of both chiral and achiral (poly)phosphines, many of which are unsurpassed as ligands for the support of transition metal catalysts.[1] These adducts are characterized by several key features: (i) the P−B bond is conveniently formed by the addition of commercially available BH$_3$·THF or BH$_3$·SMe$_2$ to the corresponding phosphine; (ii) the P−B bond is stable under a wide variety of reaction conditions, and so the phosphorus centers are effectively protected from oxidation; (iii) formation of the adduct decreases the hydridic character of the B−H hydrogen atoms, and so these compounds are relatively inert; (iv) the formation of the P−B bond is frequently reversible, and, for P-chiral adducts, cleavage of the borane group proceeds with retention of configuration at phosphorus; and (v) CH protons α to the phosphorus center are activated toward deprotonation, affording highly stabilized carbanions.

The straightforward formation and cleavage of the P−B bond under relatively mild conditions is one of the most useful of these features. For borane adducts of electron-poor phosphines, P−B cleavage may be achieved by treatment of the phosphine-borane with a large excess of amine, which acts to displace the borane group and form the corresponding amine-borane adduct,[2] or by alcoholysis of the adduct with ethanol or methanol at elevated temperatures.[3] For borane adducts of electron-rich phosphines, which are not amenable to amine- or alcohol-mediated deprotection, P−B cleavage is best achieved by treatment of the adduct with strong acids such as HBF$_4$ or HOTf.[4]

Perhaps of equal importance is the ability of phosphine-borane groups to activate an α-CH group toward deprotonation, to give the corresponding phosphine-borane-stabilized carbanion (PBC), [R$_2$P(BH$_3$)CR′$_2$]$^-$.[1] This permits the convenient elaboration of phosphine-borane adducts, providing straightforward access to an impressive diversity of functionalized mono- and diphosphines. Typically, such carbanions are generated via treatment of the phosphine-borane adduct with an organolithium reagent. In the vast majority of cases these phosphine-borane-stabilized carbanion complexes are generated and used *in situ*, and, until recently, little was known about the structures of and bonding in these species. This is particularly surprising given the isoelectronic and isosteric relationship between Me$_2$P(BH$_3$) and Me$_3$Si groups, the latter of which have played a fundamental role in the development of main group, transition metal, and lanthanide organometallic chemistry. It is noteworthy, however, that while Me$_2$P(BH$_3$) and Me$_3$Si groups bear a strong resemblance to each other, the former also afford the opportunity for the formation of

Received: June 5, 2014

   dx.doi.org/10.1021/om5005995 | *Organometallics* XXXX, XXX, XXX−XXX

moderately strong B−H···M contacts by virtue of the residual hydridic character of the H atoms in the BH_3 group. Such contacts are found in almost all of the small number of known main group, lanthanide, and transition metal complexes of PBCs, and these potentially hemilabile interactions afford a mechanism by which electron density may be donated to the metal centers.[5−7] This has proven to be a unique feature of these ligands, permitting the isolation of otherwise inaccessible compounds; for example, we have shown that B−H···E contacts significantly stabilize electron-deficient Sn(II) and Pb(II) centers, enabling the isolation of a rich variety of monomeric dialkylstannylenes and -plumbylenes R_2E (E = Sn, Pb).[7]

We now report the synthesis of a new mixed phosphine/phosphine-borane and studies on the migration of the borane group between the two phosphorus centers in this compound, including a detailed study of the kinetics of this rearrangement. We also report the metalation of both of these compounds and the corresponding bis(phosphine) and bis(phosphine-borane) and, with reference to accompanying DFT studies, comment on the relative charge-stabilizing capacity of the two phosphorus centers in each case.

RESULTS AND DISCUSSION

Phosphine-Boranes: Synthesis and Mechanistic Aspects. The low-temperature reaction between iPr_2PCl and one equivalent of *in situ* generated $Ph_2P(BH_3)CH_2Li$ in THF gives the mixed phosphine/phosphine-borane $Ph_2P(BH_3)CH_2PiPr_2$ (**1a**) as a colorless, crystalline solid in excellent yield (Scheme 1). Since the iPr_2P moiety in this compound is more electron-rich than the Ph_2P moiety, there is the potential for migration of the borane group from the latter to the former center during this reaction. However, $^{11}B\{^1H\}$ and $^{31}P\{^1H\}$ NMR spectra of the crude reaction solution confirm that **1a** is the sole phosphorus-containing product under these conditions. The $^{31}P\{^1H\}$ NMR spectrum of **1a** consists of a broad multiplet at 16.6 ppm and a sharp doublet at −8.3 ppm (J_{PP} = 73 Hz), which we assign to the phosphine-borane and tertiary phosphine centers, respectively. Selective decoupling of the ^{31}P nuclei resonating at −8.3 ppm leads to loss of ^{31}P coupling in the ^1H NMR signal due to the *i*Pr groups, while selective decoupling of the ^{31}P nuclei resonating at 16.6 ppm leads to loss of ^{31}P coupling in the aromatic region of the ^1H NMR spectrum, confirming that the borane group remains attached to the Ph_2P center in **1a**.

Although **1a** is isolated cleanly through the above procedure, the borane group slowly migrates from the Ph_2P to the more electron-rich iPr_2P center over a period of several weeks in toluene solution at room temperature, to give the alternative phosphine/phosphine-borane $Ph_2PCH_2P(BH_3)iPr_2$ (**2a**); the identity of **2a** was confirmed by multinuclear NMR spectroscopy and selective $^1H\{^{31}P\}$ NMR experiments. This rearrangement is accelerated at higher temperatures: heating a solution of **1a** in toluene under reflux for 12 h gives **2a** as a colorless oil, after removal of solvent, in excellent yield. Below 0 °C compound **1a** is stable in the solid state and shows no sign of isomerization to **2a** even after several months.

Scheme 1. Syntheses of 1a−4a

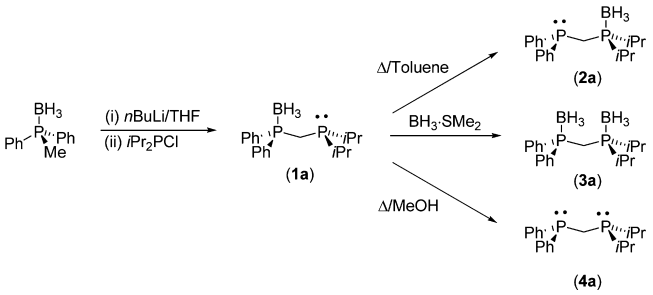

The clean isolation of **1a** provides an excellent opportunity to study the migration of a borane group between two electronically different tertiary phosphine centers in the same molecule. Perhaps surprisingly, given the ubiquity of BH_3 adducts in phosphine chemistry, previous mechanistic studies have focused on the cleavage of P−B bonds in adducts between tertiary phosphines and substituted (e.g., alkyl, aryl, or alkoxy) boranes;[8−11] to the best of our knowledge there has been no prior investigation of the mechanism by which $R_3P{-}BH_3$ bonds are cleaved by Lewis bases. This is possibly a consequence of the weaker P−B bonds, and hence more rapid exchange processes, in phosphine-organoborane adducts, which allow for straightforward investigation of exchange phenomena by variable-temperature NMR studies.

For amine-mediated P−B cleavage both dissociative (S_N1-type) and associative (S_N2-type) mechanisms have been proposed, the adopted mechanism appearing to depend on the substituents at the B center. For example, variable-temperature ^1H NMR studies on $R_3P{-}BMe_3$ and $R_3P{-}BPhMe_2$ [R_3P = Me_3P, $PhMe_2P$, $tBuMe_2P$, $Me_2(Me_2N)P$] suggest a dissociative mechanism for exchange between these adducts and an excess of either donor or acceptor.[8] In contrast, the displacement of PPh_3 from the B-chiral adduct $Ph_3P{-}BH(CN)(Ipc)$ with $PPhMe_2$ appears to proceed via a dissociative mechanism in THF, but an associative mechanism in C_6D_6 [Ipc = monoisopinocampheyl].[9] Theoretical calculations on the transfer of BH_3 between various Lewis bases indicate that the associative and dissociative processes may have almost identical free energies of activation, such that both mechanisms may operate in a single reaction.[10]

We find that heating a solution of **1a** in toluene to 80 °C results in a gradual decrease in the intensity of the $^{31}P\{^1H\}$ NMR signals due to **1a**, accompanied by the appearance of a sharp doublet at −26.7 (J_{PP} = 38 Hz) and a broad multiplet at 35.5 ppm, due to the PPh_2 and $PiPr_2$ centers of the borane-exchange product **2a** (Figure 1). In addition, after a short induction period, additional, low-intensity, broad multiplets

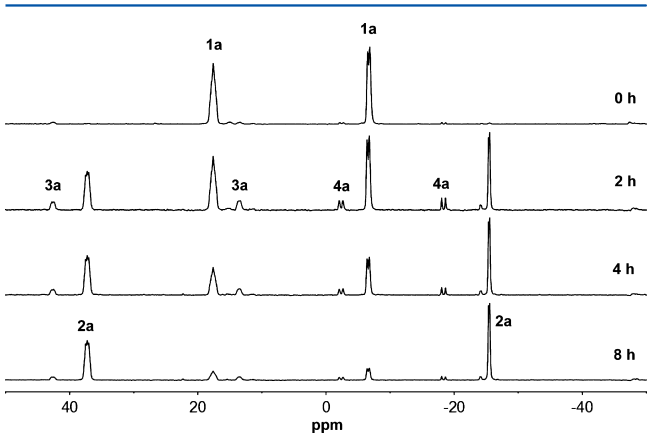

Figure 1. $^{31}P\{^1H\}$ NMR spectra of **1a** in d_8-toluene at 80 °C over 8 h.

dx.doi.org/10.1021/om5005995 | Organometallics XXXX, XXX, XXX−XXX

Scheme 2. Possible Pathways for the Migration of BH_3 between the Two Phosphorus Centers

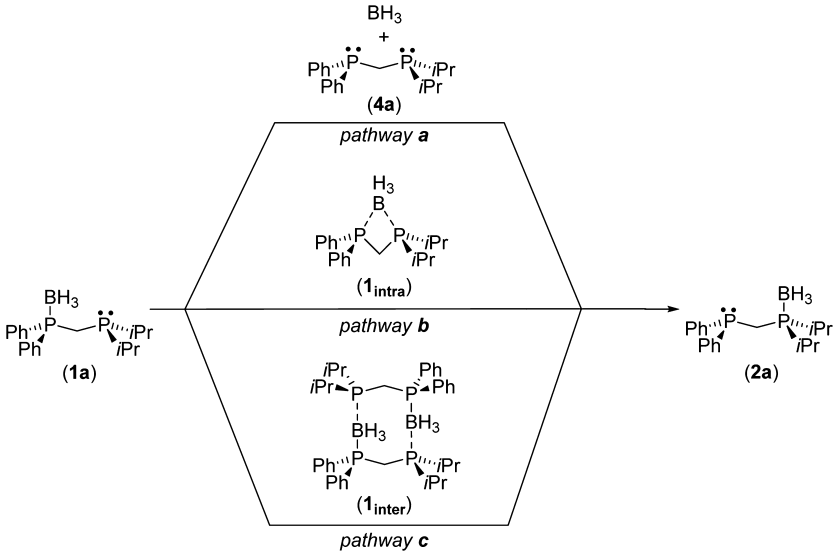

appear at 12.6 and 40.8 ppm, along with a low-intensity, sharp pair of doublets at −3.0 and −18.6 ppm (J_{PP} = 123 Hz), due to the bis(phosphine-borane) $Ph_2P(BH_3)CH_2P(BH_3)iPr_2$ (**3a**) and the bis(phosphine) $Ph_2PCH_2PiPr_2$ (**4a**), respectively; the identities of **3a** and **4a** were confirmed by comparison with data from deliberately prepared samples of these compounds (see below). At 80 °C the concentrations of **3a** and **4a** reach a maximum of 7.8% and 6.1%, respectively, after 2 h, before gradually decreasing to 5.7% and 3.4%, respectively, after 8 h. Small amounts (<1%) of **3a** and **4a** remained in samples that had been heated at this temperature for several days.

The rearrangement of **1a** to **2a** was monitored by $^{31}P\{^1H\}$ NMR spectroscopy at 5 °C intervals between 60 and 90 °C. The kinetic data obtained indicate that the reaction exhibits an apparent first-order dependence on the concentration of **1a**; consistent with this, the rate of consumption of **1a** exhibits a linear relationship with the concentration of this compound (see Supporting Information). However, the formation of **2a**, **3a**, and **4a** does not obey simple first- or second-order kinetics.

The apparent first-order dependence of the migration of BH_3 on **1a** suggests that the rate-determining step of the rearrangement of **1a** to **2a** is a unimolecular process and is consistent with either (i) an S_N1-type process involving dissociation of BH_3 from the PPh_2 group (pathway **a**, Scheme 2) or (ii) intramolecular migration of the borane group *between* the two phosphorus centers in the compound via transition state $\mathbf{1}_{intra}$ (pathway **b**). Pathway **a** is also consistent with the formation of **4a** as an intermediate in the reaction and with the formation of **3a** (from the reaction of **1a** with the free BH_3 formed during such a dissociative process). However, both the formation of **3a** and **4a** and the non-first-order kinetics for the formation of **2a** suggest that the rearrangement of **1a** to **2a** is not straightforward and that it is unlikely to proceed through a single process.

Consistent with the foregoing, while the formation of **3a** and **4a** supports a dissociative process, a plot of $\ln(k/T)$ versus $1/T$ for the decay of **1a** gives a straight line, which yields the activation parameters $\Delta H^{\ddagger}$ = 63 ± 8 kJ mol^{-1}, $\Delta S^{\ddagger}$ = −145 ± 24 J K^{-1} mol^{-1}, and $\Delta G^{\ddagger}$ = 106 ± 8 kJ mol^{-1}. The value of $\Delta H^{\ddagger}$ is rather low for a process involving the breaking of a P−B bond (the bond dissociation energy of $Me_3P{-}BH_3$ has previously been calculated as 166.5 kJ mol^{-1}),[12] while the strongly negative value of $\Delta S^{\ddagger}$ is inconsistent with a dissociative process. Rather, these values suggest either an intramolecular migration of the BH_3 group between the Ph_2P and iPr_2P moieties, via a four-membered transition state ($\mathbf{1}_{intra}$), or an intermolecular migration of BH_3 between two molecules of **1a** (via transition state $\mathbf{1}_{inter}$, pathway **c**, Scheme 2). However, the former does not explain the formation of **3a** and **4a** during the rearrangement process, while the latter is inconsistent with the first-order dependence of the reaction on the concentration of **1a**.

In an attempt to resolve this dichotomy, we have undertaken a DFT study of the rearrangement of **1a** to **2a**. A brief benchmarking exercise showed that the wB97XD functional,[13] which explicitly includes mid- to long-range dispersive interactions, outperformed both the highly parametrized M06-2X[14] and the ever-popular B3LYP[15] hybrid functionals in generating an optimized geometry for **1a** that correlated with the data obtained by X-ray crystallography (see Supporting Information). Optimizations and frequency calculations were, therefore, conducted at the wB97XD/6-311+G(d,p) level of theory[16] with solvation by toluene included implicitly using the IEF polarizable continuum model (see Experimental Section for further information).[17]

The optimized geometry of **1a′** (calculated structures are indicated throughout with a prime) shows a close correspondence with the solid-state structure of **1a**; calculated bond lengths are typically overestimated by 0.01 Å or less. The global minimum energy conformations of **1a′** and **2a′** lie relatively close in energy, with **2a′** just 12.3 kJ mol^{-1} more stable than **1a′** (Figure 2).

A relaxed potential energy surface scan indicates that dissociation of BH_3 from **1a′** (pathway **a**) proceeds smoothly and does not pass through a saddle point. The calculated free energy of dissociation of the BH_3 fragment from **1a′**, corrected for basis set superposition error (BSSE), is 106.4 kJ mol^{-1}, extremely close to the experimentally determined free energy of activation for the isomerization of **1a** to **2a** (106 ± 8 kJ mol^{-1}), again suggesting that this is the likely rate-determining step in the BH_3 migration process (Figure 3); however, the enthalpy and entropy of activation for this process are 152.4 kJ mol^{-1}

dx.doi.org/10.1021/om5005995 | *Organometallics* XXXX, XXX, XXX−XXX

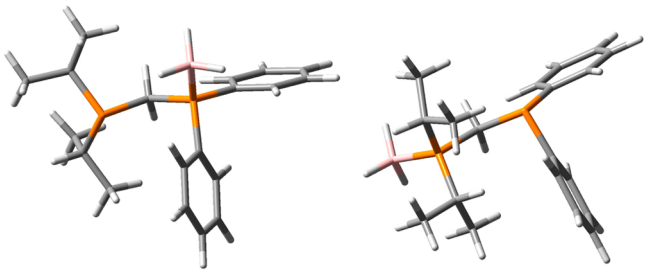

(1a′) (2a′)

Figure 2. Optimized global minimum energy geometries for **1a′** and **2a′** [wB97XD/6-311+G(d,p)].

and 154.2 J K^{-1} mol^{-1}, respectively (cf. 63 ± 8 kJ mol^{-1} and −145 ± 24 J K^{-1} mol^{-1}, respectively, for the experimentally determined values).

For comparison, a transition state ($\mathbf{1}_{intra}$′) was located for the concerted migration of the borane group between the two phosphorus centers in **1a′** (pathway **b**). The calculated free energy barrier to BH_3 migration via this transition state is 134.8 kJ mol^{-1}, suggesting that such a process is significantly disfavored with respect to dissociation of BH_3 from **1a′**. The enthalpy and entropy of activation for this process were calculated to be 141.1 kJ mol^{-1} and 21.0 J K^{-1} mol^{-1}, respectively.

We were unable to locate a stable transition state for the simultaneous migration of the two borane groups between two head-to-tail molecules of **1a′**, which would generate two

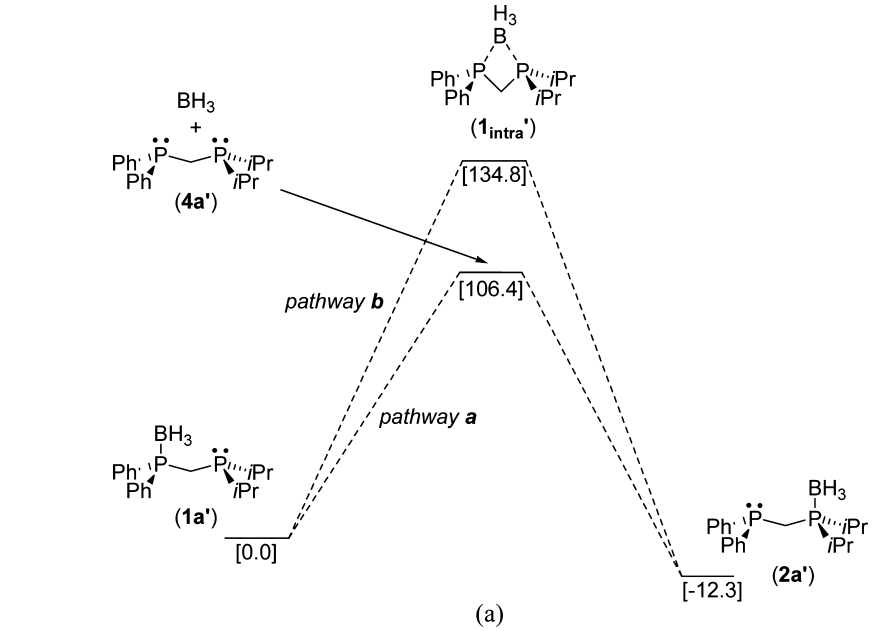

(a)

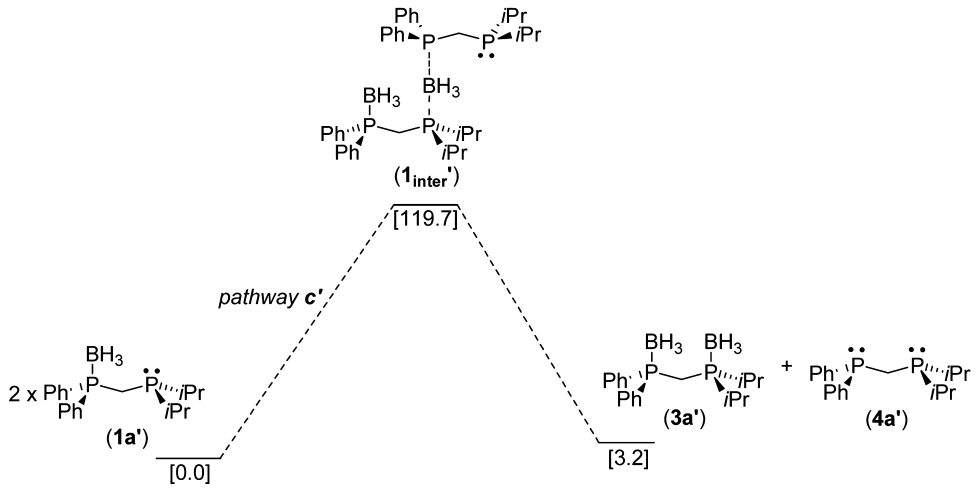

(b)

Figure 3. Relative free energies (kJ mol^{-1}) of (a) the dissociative and concerted migration pathways for conversion of **1a′** to **2a′** (pathways **a** and **b**) and (b) the associative pathway for conversion of **1a′** to a mixture of **3a′** and **4a′** (pathway **c′**) [wB97XD/6-311+G(d,p) at 298.15 K, corrected for ZPE and BSSE as appropriate].

dx.doi.org/10.1021/om5005995 | *Organometallics* XXXX, XXX, XXX−XXX

Scheme 3. Alternative Pathway to 2a via BH_3 Elimination from 3a

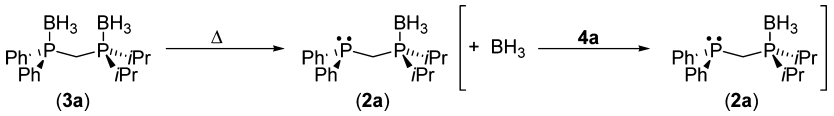

molecules of **2a′** directly (pathway **c**, see Scheme 2). However, we have modeled this process in a "slipped head-to-tail" pair, where a single BH_3 group migrates between two molecules of **1a′** to give a molecule each of **3a′** and **4a′** (pathway **c′**). The overall energy difference between two molecules of **1a′** and a molecule each of **3a′** and **4a′** is just 3.2 kJ mol^{-1}, suggesting that this process will be reversible and, therefore, that, given a sufficiently low barrier to activation, these species will be in dynamic equilibrium. The transition state for this process (**1_{inter}′**, Figure 3b) has a calculated free energy of activation of 119.7 kJ mol^{-1}. This is again close to the experimentally observed free energy of activation for the borane migration process (106 ± 8 kJ mol^{-1}), while the calculated enthalpy and entropy of activation ($\Delta H^{\ddagger}$ = +57.2 kJ mol^{-1}, $\Delta S^{\ddagger}$ = −195.7 J K^{-1} mol^{-1}) are also of a similar magnitude to the experimentally determined values ($\Delta H^{\ddagger}$ = +63 ± 8 kJ mol^{-1}, $\Delta S^{\ddagger}$ = −145 ± 24 J K^{-1} mol^{-1}). Such an intermolecular process would also account for the formation of **3a** and **4a** during the isomerization of **1a** to **2a**. However, this process is inconsistent with the apparent first-order dependence on the concentration of **1a** observed experimentally.

From the foregoing, we may reasonably rule out an intramolecular migration of the borane group (via transition state **$1_{intra'}$**) as the principal mechanism for the transformation of **1a′** into **2a′**, on the grounds of the rather large calculated free energy of activation for this process compared to the alternatives. However, both dissociation of borane from **1a′** and migration of borane between two molecules of **1a′** have similar free energies of activation (106.4 and 119.7 kJ mol^{-1}, respectively), and both lie close to the experimentally determined value of 106 ± 8 kJ mol^{-1}. It is likely, therefore, that both processes operate simultaneously and that the observed kinetic data (i.e., an apparent first-order dependence on the concentration of **1a**, but a strongly negative entropy of activation) represent a weighted average for these. This interpretation is consistent with earlier investigations into the substitution behavior of related amine-boranes, where, for adducts containing moderately sterically hindered borane moieties, S_N1 and S_N2 processes have been observed to operate simultaneously.[11]

In reality, the situation is likely to be even more complex, as these processes may be supplemented by dissociation of BH_3 from the small quantity of **3a** produced as an intermediate by pathway **c**, to give **2a** and free BH_3, the latter of which may combine with **4a** to give a further equivalent of **2a** (Scheme 3). A relaxed potential energy surface scan indicates that this dissociation proceeds smoothly and does not pass through a saddle point; the free energy for this process is calculated to be 100.3 kJ mol^{-1} (corrected for BSSE), indicating that the dissociation of **3a** is competitive with the other processes outlined above.

A clean sample of **3a** was prepared by treatment of **1a** with one equivalent of $BH_3{\cdot}SMe_2$ in THF and was isolated as an essentially pure, colorless powder on removal of the solvent. The bis(phosphine) **4a** was prepared by heating **1a** under reflux in degassed methanol for 24 h and was isolated as a colorless oil on removal of the solvent. When this latter reaction was carried out in the higher boiling ethanol, a mixture of **4a**, **3a**, and **2a** was isolated in the approximate ratio of 4:1:2, due to competitive migration of the borane group under these conditions. Since "free" BH_3 is likely to react rapidly with ethanol under these conditions, the formation of **2a** and **3a** in this reaction is further evidence for at least a second borane migration pathway, in addition to an S_N1-type dissociation of BH_3 from **1a**.

The ^1H, $^{13}C\{^1H\}$, $^{31}P\{^1H\}$, and $^{11}B\{^1H\}$ NMR spectra of both **3a** and **4a** are as expected: the $^{31}P\{^1H\}$ NMR spectrum of **3a** consists of a pair of broad multiplets at 12.6 and 40.8 ppm, while the $^{31}P\{^1H\}$ NMR spectrum of **4a** consists of a pair of doublets at −19.2 and −3.8 ppm (J_{PP} = 123 Hz). Both **3a** and **4a** were isolated cleanly from these reactions and were used without further purification.

Phosphine-Borane-Stabilized Carbanions: Synthesis, Structures, and Stabilities. Treatment of each of **1a**−**4a** with one equivalent of *n*BuLi in THF, followed by one equivalent of tmeda gives the complexes $[\{Ph_2P(BH_3)\}CHPiPr_2]Li(tmeda)$ (**1b**), $[Ph_2PCH\{P(BH_3)iPr_2\}]Li(tmeda)$ (**2b**), $[\{Ph_2P(BH_3)\}CH\{P(BH_3)iPr_2\}]Li(tmeda)$ (**3b**), and $[Ph_2PCHPiPr_2]Li(tmeda)$ (**4b**), respectively, as colorless to yellow, crystalline solids in good yield; the alternative adduct $[\{Ph_2P(BH_3)\}CHPiPr_2]Li(THF)_2$ (**1c**) was also isolated as X-ray quality crystals [tmeda = *N*,*N*,*N*′,*N*′-tetramethylethylenediamine].

The ^1H, $^{13}C\{^1H\}$, $^{11}B\{^1H\}$, $^{31}P\{^1H\}$, and $^{7}Li\{^1H\}$ NMR spectra of **1c** in d_8-toluene are as expected; the $^{7}Li\{^1H\}$ NMR spectrum consists of a singlet at 0.3 ppm, while the $^{31}P\{^1H\}$ NMR spectrum consists of a doublet (J_{PP} = 166 Hz) at 9.1 and a broad multiplet (J_{PB} = 91 Hz) at 14.1 ppm, $^{31}P-^{7}Li$ coupling is not observed due to rapid P−Li exchange on the NMR time-scale. However, the $^{7}Li\{^1H\}$ and $^{31}P\{^1H\}$ NMR spectra of **1b** in d_8-toluene consist of a broad doublet (J_{PLi} = 53 Hz) at 0.8 ppm and a pair of multiplets at 9.1 (J_{PP} = 165, J_{PLi} = 53 Hz) and 13.9 ppm (J_{PP} = 165, J_{PB} = 94 Hz), attributed to the $PiPr_2$ and $P(BH_3)Ph_2$ groups, respectively (Figure 4). The presence of $^{7}Li-^{31}P$ coupling indicates that P−Li exchange is slow on the NMR time-scale and suggests that the molecular structure of **1b** is maintained in solution. Similarly, the $^{7}Li\{^1H\}$ and $^{31}P\{^1H\}$ spectra of **2b** consist of a broad doublet at 0.9 ppm (J_{PLi} = 62 Hz) and a pair of approximate doublets of quartets at −6.7 (J_{PP} = 165, J_{PLi} = 62 Hz) and 32.2 ppm (J_{PP} = 165, J_{PB} = 95 Hz), respectively, again indicating slow P−Li exchange on the NMR time-scale. The slow P−Li exchange in these compounds clearly derives from the incorporation of the tertiary phosphine center into a chelate ligand and the partial delocalization of charge from the carbanion center onto the phosphorus atom (see below), which enhances the essentially electrostatic P−Li interaction. The ^1H, $^{13}C\{^1H\}$, $^{11}B\{^1H\}$, $^{31}P\{^1H\}$, and $^{7}Li\{^1H\}$ NMR spectra of **3b** and **4b** are as expected.

While **1a** converts slowly to **2a** on heating, we find that **1b** is unchanged after heating under reflux in toluene for several days. The P−B bond in **1b** is likely to be relatively unaffected by any negative hyperconjugation of the carbanion lone pair, and so the P−B bond strength in **1b** should be similar to that in **1a**

dx.doi.org/10.1021/om5005995 | *Organometallics* XXXX, XXX, XXX−XXX

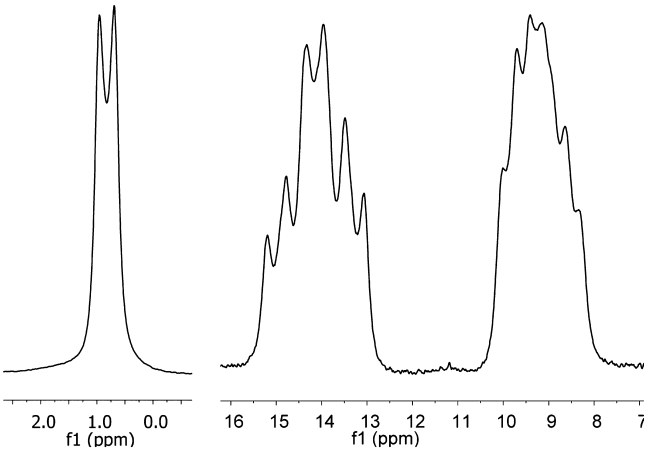

Figure 4. (a) $^{7}Li\{^{1}H\}$ and (b) $^{31}P\{^{1}H\}$ NMR spectra of **1b** in d_8-toluene.

(see DFT studies below). We therefore attribute the lack of borane migration observed on heating **1b** to the unavailability of the P*i*Pr$_2$ lone pair, which remains coordinated to the lithium cation in toluene solution. This hypothesis is supported by the slow rate of P−Li exchange evident from the $^{31}P\{^{1}H\}$ and ^{7}Li NMR spectra of **1b** (see above). Interestingly, we observe no evidence for the migration of the borane group from phosphorus to the carbanion center, such as that recently reported by Langer and co-workers for a barium complex of a phosphine-borane-stabilized carbanion.[18]

Compounds **1b**, **1c**, **2b**, **3b**, and **4b** were obtained as single crystals suitable for X-ray crystallography. These compounds present a unique opportunity to examine the effect of the degree of borane substitution and the nature of the substituents at phosphorus on the stabilities and structures of PBCs. Only the structures of the directly comparable compounds **1b**−**4b** are discussed in detail here; details of the structures of **1a** and of the THF adduct **1c** may be found in the Supporting Information.

The molecular structures of **1b** and **2b** are shown in Figure 5, along with selected bond lengths and angles. Compounds **1b** and **2b** crystallize as discrete molecular species. In each case the lithium ions are coordinated by the two nitrogen atoms of a chelating molecule of tmeda and by the tertiary phosphine center and an η^2-BH$_3$ contact with the phosphine/phosphine-borane-stabilized carbanion. This affords a distorted pseudotetrahedral geometry at the lithium centers and generates a pseudo-five-membered Li−P−C−P−B ring in each case. There is no contact in each case between the lithium cations and the formal carbanion centers. The Li−P distances in **1b** and **2b** of 2.621(3) and 2.583(3) Å, respectively, are typical of Li−P distances in lithium phosphinomethanides;[19] for example, the Li−P distances in $[\{(Me_2PhSi)(Me_2P)_2C\}Li]_3$ range from 2.573(7) to 2.641(7) Å.[20] The Li−H and Li···B distances in **1b** [Li−H 1.97(2) and 2.20(2) Å, Li···B 2.442(4) Å] and **2b** [Li−H 1.923(18) and 2.043(17) Å, Li···B 2.361(3) Å] are typical of η^2-BH$_n$−Li contacts; for example, the Li−H and Li···B distances in $[\{Me_2P(BH_3)\}Li(tmeda)]_\infty$ are 2.03(2) and 2.372(4) Å, respectively.[21] For comparison, the Li−H distances in [Li(BH$_4$)(pmdeta)], in which the BH$_4$ anions adopt an η^2 configuration, are 2.04(4) and 2.05(4) Å,[22a] while the Li−H distances in $[Li(BH_4)(tmeda)]_2$, in which the BH$_4$ anion

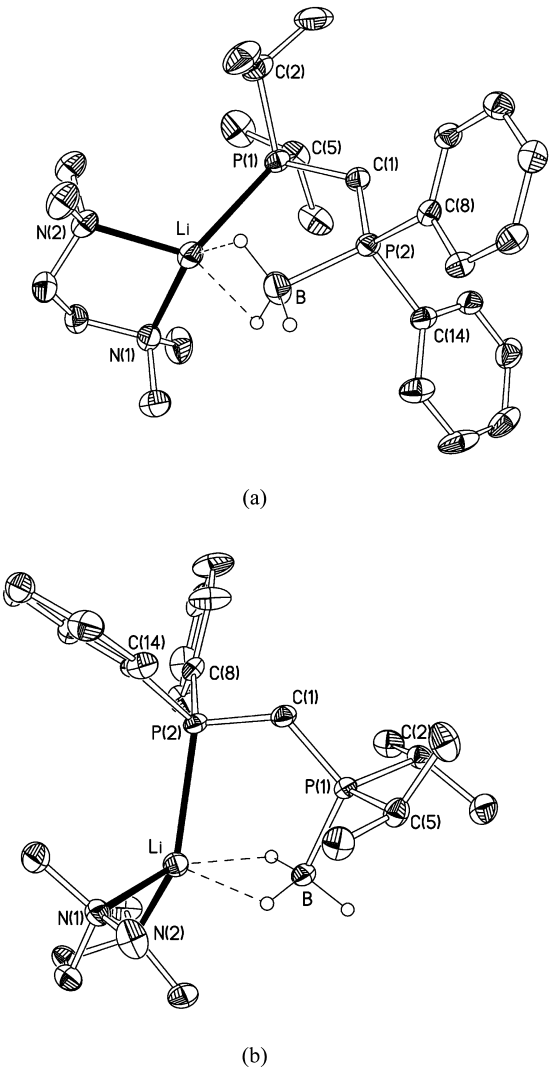

Figure 5. Molecular structures of (a) **1b** and (b) **2b**, with 40% probability ellipsoids and with C-bound H atoms omitted for clarity. Selected bond lengths (Å) and angles (deg): **1b** Li−P(1) 2.583(3), Li−N(1) 2.145(4), Li−N(2) 2.086(4), Li−H(B) 2.20(2), Li−H(C) 1.97(2), Li···B 2.442(4), P(1)−C(1) 1.736(2), P(1)−C(2) 1.869(2), P(1)−C(5) 1.856(2), P(2)−B 1.933(2), P(2)−C(1) 1.702(2), P(2)−C(8) 1.8305(19), P(2)−C(14) 1.842(2), P(1)−Li···B 86.91(12), P(1)−C(1)−P(2) 120.83(12); **2b** Li−P(2) 2.621(3), Li−N(1) 2.128(3), Li−N(2) 2.088(3), Li−H(A) 2.043(17), Li−H(B) 1.923(18), Li···B 2.361(3), P(1)−B 1.925(2), P(1)−C(1) 1.7158(15), P(1)−C(2) 1.8494(16), P(1)−C(5) 1.8409(17), P(2)−C(1) 1.7292(17), P(2)−C(8) 1.8439(16), P(2)−C(14) 1.8438(16), P(2)−Li···B 86.72(10), P(1)−C(1)−P(2) 120.76(9).

adopts a μ_2-η^3:η^3 bridging mode, range between 2.02(3) and 2.12(3) Å, and the Li···B distances in this compound are 2.467(5) and 2.461(6) Å [pmdeta = *N*,*N*,*N*′,*N*″,*N*″-pentamethyldiethylenetriamine].[22b]

Compound **3b** crystallizes with two independent molecules in the asymmetric unit, which differ only marginally in structure; the structure of **3b** is shown in Figure 6, along with selected bond lengths and angles. Each lithium cation is coordinated by the two N atoms of a chelating molecule of tmeda and by two η^2-BH$_3$ contacts; once again there is no contact between the lithium ion and the formal carbanion center. This affords a pseudotetrahedral geometry at lithium and generates a pseudo-six-membered Li−B−P−C−P−B

dx.doi.org/10.1021/om5005995 | *Organometallics* XXXX, XXX, XXX−XXX

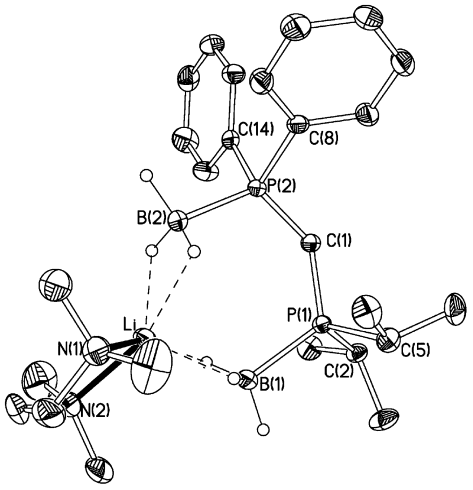

Figure 6. Molecular structure of one of the two independent molecules of **3b** with 40% probability ellipsoids and with C-bound H atoms omitted for clarity. Selected bond lengths (Å) and angles (deg): molecule 1 Li−H(1A) 1.927(17), Li−H(1C) 2.079(18), Li−H(2A) 2.082(17), Li−H(2B) 2.007(17), Li−N(1) 2.102(3), Li−N(2) 2.115(3), Li···B(1) 2.402(3), Li···B(2) 2.424(3), P(1)−B(1) 1.9335(18), P(1)−C(1) 1.7242(16), P(1)−C(2) 1.8445(16), P(1)−C(5) 1.8487(17), P(2)−B(2) 1.9285(18), P(2)−C(1) 1.7061(16), P(2)−C(8) 1.8342(16), P(2)−C(14) 1.8326(16), B(1)···Li···B(2) 95.29(11), P(1)−C(1)−P(2) 129.22(9); molecule 2 Li(2)-H(3A) 2.051(19), Li(2)−H(3B) 1.941(19), Li(2)−H(4A) 2.007(17), Li(2)−H(4B) 2.092(17), Li(2)−N(3) 2.125(3), Li(2)−N(4) 2.113(3), Li(2)···B(3) 2.418(3), Li(2)···B(4) 2.439(3), P(3)−B(3) 1.9308(19), P(3)−C(26) 1.7223(17), P(3)−C(27) 1.8411(17), P(3)−C(30) 1.8454(17), P(4)−B(4) 1.9290(18), P(4)−C(26) 1.7070(16), P(4)−C(33) 1.8359(16), P(3)−C(39) 1.8304(16), B(3)···Li(2)···B(4) 94.75(11), P(3)−C(26)−P(4) 128.89(10).

chelate ring. The Li−H distances range from 1.927(17) to 2.092(17) Å, while the Li···B distances range from 2.402(3) to 2.439(3) Å, consistent with an η^2-BH_3−Li contact (see above). These distances are similar to the Li−H and Li···B distances in the related compound $[\{Ph_2P(BH_3)\}_2CH]Li(OEt_2)_2$, which also exhibits η^2-BH_3−Li contacts.[5j]

Compound **4b** adopts a typical structure for a diphosphinomethanide complex; the molecular structure of **4b** is shown in Figure 7, along with selected bond lengths and angles. The lithium ion is coordinated by both of the phosphorus centers to give a four-membered chelate ring [bite angle 70.09(10)°] and by the two nitrogen atoms of the tmeda coligand, affording an approximately tetrahedral geometry at the lithium center. In addition, the lithium ion has short contacts with both of the methylene carbon atoms of the tmeda coligand [Li···C(22) 2.786(4), Li···C(23) 2.760(4) Å]. The two Li−P distances are rather similar [Li−P(1) 2.537(4), Li−P(2) 2.568(4) Å] and are typical of Li−P distances in lithium phosphinomethanide complexes.[19]

Although the precise location of hydrogen atom positions is problematic, the carbanion centers in **1b**−**4b** appear to adopt a planar configuration [sums of angles at C(1) = 358.39−359.96°]. The P−C−P angle increases with increasing borane substitution of the PBC ligand [P(1)−C(1)−P(2) 115.54(11)° (**4b**), 120.83(12)° (**1b**), 120.76(9)° (**2b**), 129.22(9)°/128.89(10)° (**3b**)], consistent with the increase in steric compression in each case and the change in chelate ring size from a four- to a pseudo-five- to a pseudo-six-membered ring on going from **4b** to **1b**/**2b** to **3b**, respectively.

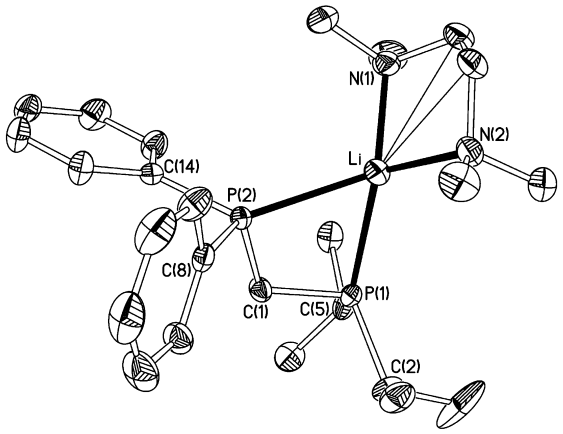

Figure 7. Molecular structure of **4b** with 40% probability ellipsoids and with C-bound H atoms omitted for clarity. Selected bond lengths (Å) and angles (deg): Li−P(1) 2.537(4), Li−P(2) 2.568(4), Li−N(1) 2.080(4), Li−N(2) 2.073(4), Li···C(22) 2.786(4), Li···C(23) 2.760(4), P(1)−C(1) 1.738(2), P(1)−C(2) 1.870(2), P(1)−C(5) 1.867(2), P(2)−C(1) 1.7277(19), P(2)−C(8) 1.844(2), P(2)−C(14) 1.853(2), P(1)−Li−P(2) 70.09(10), P(1)−C(1)−P(2) 115.54(11).

Metalation of **1a** results in a significant decrease in the C(1)−P(1) and C(1)−P(2) distances [C(1)−P(1) 1.867(4) (**1a**), 1.736(2) Å (**1b**); C(1)−P(2) 1.815(5) (**1a**), 1.701(2) Å (**1b**)], consistent with the change in hybridization of C(1) from sp^3 to sp^2 and with partial C(1)−P multiple-bond character due to the delocalization of charge from the carbanion center into the P−C σ^*-orbitals (negative hyperconjugation). Consistent with this, the C(1)−P(1) and C(1)−P(2) distances in **2b**, **3b**, and **4b** are also significantly shorter than the corresponding distances in **1a** (see Table 1).

The C(1)−P(1) distance in **1a** [1.867(4) Å] is significantly longer than the C(1)−P(2) distance [1.815(5) Å], possibly as a consequence of the inductive effect of the propyl groups, which decreases the electronegativity, and therefore increases the covalent radius, of P(1) in comparison to P(2). A similar, although less pronounced, difference is seen for the corresponding distances in the lithium complex **1b**, the bis(phosphine-borane)-stabilized carbanion complex **3b**, and the bis(phosphino)methanide complex **4b**. In contrast, for **2b**, in which there is a single borane group on the iPr$_2$P center, the C(1)−P(2) distance [1.7292(17) Å] is longer than the C(1)−P(1) distance [1.7158(15) Å]. This suggests that there is greater delocalization of electron density from the carbanion center toward a phosphine-borane, rather than a phosphine group; this is supported by our DFT calculations (see below).

DFT Studies on PBC Complexes. The closely related series of complexes **1b**−**4b** provides a unique opportunity to investigate the extent of negative hyperconjugation in phosphine- and phosphine-borane-stabilized carbanions and provides insight into the molecular orbitals involved: each of these compounds has the same coligand (tmeda) and adopts a similar structure, with solely Li−P and/or Li···BH_3 contacts between the lithium cation and the corresponding anion.

The calculated structures of **1b′**−**4b′** bear a very close resemblance to the structures obtained by X-ray crystallography; at the wB97XD/6-311+G(d,p) level of theory bond lengths in the calculated structures are typically overestimated by 0.02 Å or less. The calculated changes in geometric parameters on metalation of the free phosphine-boranes **1a′**−**4a′** are consistent with the observed differences between the

dx.doi.org/10.1021/om5005995 | Organometallics XXXX, XXX, XXX−XXX

Table 1. Selected Bond Lengths (Å) and Angles (deg) for 1a and 1b−4b

	1a	1b	2b	3b	4b
P(1)−B(1)			1.925(2)	1.9335(18)	
P(2)−B(2)	1.913(6)	1.933(2)		1.9285(18)	
C(1)−P(1)	1.867(4)	1.736(2)	1.7158(15)	1.7242(16)	1.738(2)
C(1)−P(2)	1.815(5)	1.701(2)	1.7292(17)	1.7061(16)	1.7277(19)
C(2)−P(1)	1.869(5)	1.869(2)	1.8494(16)	1.8445(16)	1.870(2)
C(5)−P(1)	1.854(4)	1.856(2)	1.8409(17)	1.8487(17)	1.867 (2)
C(8)−P(2)	1.820(4)	1.8305(19)	1.8439(16)	1.8342(16)	1.844(2)
C(14)−P(2)	1.814(4)	1.842(2)	1.8438(16)	1.8326(16)	1.853(2)
P(1)−C(1)−P(2)	99.3(2)	120.83(12)	120.76(9)	129.22(9)	115.54(11)

Table 2. Comparison of Calculated Bond Lengths (Å) and Angles (deg) on Metalation of the Free Phosphine-Boranes

	1a′	Δ	1b′	2a′	Δ	2b′	3a′	Δ	3b′	4a′	Δ	4b′
P(1)−B(1)				1.9301	*+0.0133*	1.9434	1.9322	*+0.0061*	1.9383			
P(2)−B(2)	1.9281	*+0.0159*	1.9440				1.9327	*+0.0022*	1.9349			
C(1)−P(1)	1.8802	*−0.1281*	1.7521	1.8366	*−0.1064*	1.7302	1.8505	*−0.1123*	1.7382	1.8735	*−0.1188*	1.7547
C(1)−P(2)	1.8271	*−0.1094*	1.7177	1.8588	*−0.1239*	1.7349	1.8335	*−0.1118*	1.7217	1.8549	*−0.1197*	1.7352
C(2)−P(1)	1.8731	*−0.0034*	1.8697	1.8442	*+0.0158*	1.8600	1.8498	*+0.0132*	1.8630	1.8727	*−0.0005*	1.8722
C(5)−P(1)	1.8680	*+0.0158*	1.8838	1.8495	*+0.0147*	1.8642	1.8476	*+0.0109*	1.8585	1.8688	*+0.0138*	1.8826
C(8)−P(2)	1.8219	*+0.0173*	1.8392	1.8424	*+0.0084*	1.8508	1.8150	*+0.0330*	1.8480	1.8471	*+0.0078*	1.8549
C(14)−P(2)	1.8236	*+0.0233*	1.8469	1.8449	*+0.0097*	1.8546	1.8272	*+0.0098*	1.8370	1.8435	*+0.0114*	1.8568
P(1)−C(1)−P(2)	112.50	*+7.04*	119.54	121.12	*−0.32*	120.80	125.20	*+2.53*	127.73	110.94	*+4.68*	115.62

Table 3. $E(2)$ Energies (kJ mol^{-1}) of Selected Delocalizations, the Percentage p-Character of the Carbon Lone Pair, and Its Occupancy for 1b′−4b′

	1b′	sum	2b′	sum	3b′	sum	4b′	sum
l.p.C(1)→P(1)−B(1)	–		0.00		5.77		–	
l.p.C(1)→P(2)−B(2)	0.00		–		3.26		–	
l.p.C(1)→P(1)−C(2)	35.90	105.40	55.15	133.64	97.78	119.12	31.25	112.46
l.p.C(1)→P(1)−C(5)	69.50		78.49		21.34		81.21	
l.p.C(1)→P(2)−C(8)	52.84	146.65	40.59	121.72	98.03	133.09	47.66	132.55
l.p.C(1)→P(2)−C(14)	93.81		81.13		35.06		84.89	
%p char l.p.C(1)	97.5		99.1		96.7		98.7	
occupancy l.p.C(1)	1.68		1.69		1.71		1.65	

Table 4. Wiberg Bond Indices for 1a′−4a′ and 1b′−4b′

	1a′	Δ	1b′	2a′	Δ	2b′	3a′	Δ	3b′	4a′	Δ	4b′
P(1)−B(1)				0.970	*−0.007*	0.963	0.975	*−0.007*	0.968			
P(1)-Li			0.325									0.315
P(2)−B(2)	0.961	*−0.008*	0.953				0.965	*−0.006*	0.959			
P(2)−Li						0.013						0.271
C(1)−P(1)	0.883	0.196	1.079	0.910	0.203	1.103	0.885	0.184	1.069	0.903	0.198	1.101
C(1)−P(2)	0.923	0.222	1.145	0.910	0.219	1.119	0.903	0.209	1.112	0.924	0.228	1.152
C(2)−P(1)	0.907	*−0.043*	0.864	0.893	*−0.047*	0.846	0.899	*−0.057*	0.832	0.907	*−0.044*	0.863
C(5)−P(1)	0.904	*−0.058*	0.846	0.896	*−0.058*	0.838	0.899	*−0.026*	0.873	0.901	*−0.065*	0.836
C(8)−P(2)	0.897	*−0.043*	0.854	0.911	*−0.031*	0.880	0.909	*−0.076*	0.833	0.911	*−0.042*	0.869
C(14)−P(2)	0.904	*−0.076*	0.828	0.926	*−0.077*	0.849	0.900	*−0.030*	0.870	0.922	*−0.079*	0.843

solid-state structures of **1a** and **1b**. In each case metalation leads to a significant decrease in the C(1)−P distances of between 0.11 and 0.13 Å (Table 2). While some of this decrease may be attributed to the smaller covalent radius of the sp^2-hybridized carbanion center in **1b′** compared to the sp^3-hybridized methylene carbon in **1a′**, and to an increased electrostatic interaction between the negatively charged carbanion center and the partially positively charged phosphorus atom in the P(BH$_3$) center in **1b′**, natural bond orbital (NBO) analyses[23] indicate substantial C−P multiple-bond character in the anions due to delocalization of the carbanion lone pair into the P−C σ*-orbitals. NBO analyses of **1b′**−**4b′** reveal that the HOMO is a lone pair at carbon, which has >96% p-character in each case, and that this is extensively delocalized into the P−C(Ph) and P−C(Pr) σ*-orbitals. This $C_{l.p.} \rightarrow (P-C)^*$ negative hyperconjugation is significantly stabilizing, such that the $E(2)$

dx.doi.org/10.1021/om5005995 | Organometallics XXXX, XXX, XXX−XXX

energies of these interactions lie between 21.3 and 98.0 kJ mol^{-1} (Table 3); in each case, the greatest stabilization is observed where the acceptor antibonding orbital is aligned with the lone pair orbital at the carbanion center, as expected. In accord with the foregoing, the Wiberg bond indices (WBIs) for the C(1)−P bonds increase significantly (by between 0.184 and 0.228) on metalation (Table 4). Since the borane group coordinates the lithium ion in each of **1b′**−**3b′**, the p-type carbanion lone pair lies orthogonal to the plane of the P−B σ*-orbital, and so there is essentially no hyperconjugation between these orbitals and, correspondingly, only a marginal change in P−B WBI on metalation of the neutral precursors.

These observations are in agreement with So and Mézailles' recent study of the isolated mono- and dicarbanions $[Ph_2P(S)CHP(BH_3)Ph_2]^-$ and $[Ph_2P(S)CHP(BH_3)Ph_2]^{2-}$, in which the major negative hyperconjugative interactions were found to be between the (di)carbanion lone pair(s) and the P(S)−C(Ph) σ*-orbitals, with smaller, but still significant delocalizations into the P(BH$_3$)−C(Ph) σ*-orbitals.[24] In the present case, the greatest delocalizations are observed to the P(BH$_3$)−C(Ph/Pr) σ*-orbitals.

The present study allows for a direct comparison between the degree of negative hyperconjugation supported by an adjacent phosphine-borane group in contrast to an adjacent phosphine substituent. In **3b′** and **4b′**, which possess either two phosphine-borane or two phosphine groups, respectively, it is notable that there is a greater degree of negative hyperconjugation into the P−C(Ph) compared to the P−C(Pr) σ*-orbitals in each case [the sum of $E(2)$ energies for the pair of interactions is 133.09 and 119.12 kJ mol^{-1}, respectively, for **3b′** and 132.55 and 112.46 kJ mol^{-1} for **4b′**]. This is consistent with a better energy match between the lone pair orbitals and the P−C(Ph) σ*-orbitals in each case. In addition to this, in **1b′** and **2b′**, where only one of the phosphorus atoms is bound to a borane group, the carbanion electron density is more extensively delocalized into the P−C σ*-orbitals of the phosphine-borane substituent in comparison to the phosphine substituent. For example, in **1b′** the sum of the $E(2)$ energies of the $C_{l.p.}$ → (P(BH$_3$)−C)* delocalizations is 146.65 kJ mol^{-1}, whereas the sum of these energies for the $C_{l.p.}$ → (P−C)* delocalizations is 105.40 kJ mol^{-1}. For **2b′** there is at first glance a less substantial difference in the $E(2)$ energies of the $C_{l.p.}$ → (P(BH$_3$)−C)* and $C_{l.p.}$ → (P−C)* delocalizations [133.64 and 121.72 kJ mol^{-1}, respectively]; however, the underlying difference is masked by the greater delocalization of electron density into the P−C(Ph) compared to the P−C(Pr) σ*-orbitals in all of **1b′** to **4b′**.

Consistent with the foregoing, in almost all cases metalation of **1a′**−**3a′** results in a small increase in the P−C(Ph) and P−C(Pr) distances of up to 0.034 Å, with a corresponding decrease in WBI of between 0.026 and 0.079; in each case the greatest increase in bond length/decrease in WBI is observed in the P(BH$_3$)−C(Ph/Pr) bond in the substituent that lies pseudoantiperiplanar to the carbanion lone pair. In contrast, metalation has little effect on the P−B distance(s), which increase by approximately 0.01 Å in each case, with a corresponding decrease in WBI of between 0.006 and 0.008; NBO analysis similarly indicates there is essentially no interaction between the lone pair at carbon and the P−B σ*-orbital(s) (the $E(2)$ energies for this interaction range between 0.00 and 5.77 kJ mol^{-1}).

CONCLUSIONS

The clean synthesis of the mixed phosphine/phosphine-borane adduct **1a** provides ready access to the corresponding isomer **2a**, the bis(phosphine-borane) **3a**, and the unsymmetrical bis(phosphine) **4a**. Detailed kinetic and DFT studies reveal that the thermally driven isomerization of **1a** into **2a** is not straightforward, but appears to proceed via at least two mechanisms simultaneously: (i) slow dissociation of BH$_3$ from the Ph$_2$P center in **1a**, followed by rapid adduct formation between the released BH$_3$ and the *i*Pr$_2$P center, and (ii) intermolecular migration of BH$_3$ between two molecules of **1a**. These processes may additionally be supplemented by the dissociation of BH$_3$ from the bis(phosphine-borane) **3a**.

Analysis of the solid-state structures of the lithium salts **1b**−**4b** indicates that the phosphine/phosphine-borane-stabilized carbanions are significantly stabilized by delocalization of the carbanion lone pair into the P−C σ*-orbitals. DFT calculations and NBO analyses support this proposal and indicate that the greatest delocalization is into the P−C σ*-orbitals of the phosphine-borane substituent in each case.

EXPERIMENTAL SECTION

All manipulations were carried out using standard Schlenk techniques under an atmosphere of dry nitrogen. THF, toluene, and diethyl ether were dried prior to use by distillation under nitrogen from sodium, potassium, or sodium/potassium alloy as appropriate; CH_2Cl_2 and hexamethyldisiloxane were distilled from CaH_2 under nitrogen. THF, CH_2Cl_2, and hexamethyldisiloxane were stored over activated 4A molecular sieves; all other solvents were stored over a potassium film. Deuterated toluene and C_6D_6 were distilled from potassium and $CDCl_3$ was distilled from CaH_2 under nitrogen; all NMR solvents were deoxygenated by three freeze−pump−thaw cycles and were stored over activated 4A molecular sieves. $Ph_2P(BH_3)Me$ was prepared by a previously published procedure;[25] *n*-butyllithium was purchased from Aldrich as a 2.5 M solution in hexanes. Tmeda was distilled from CaH_2 under nitrogen and was stored over activated 4A molecular sieves. All other compounds were used as supplied by the manufacturer.

^{1}H and ^{13}C{^{1}H} NMR spectra were recorded on a JEOL ECS500 spectrometer operating at 500.16 and 125.65 MHz, respectively, a JEOL ECS400 spectrometer operating at 399.78 and 100.53 MHz, respectively, or a Bruker Avance300 spectrometer operating at 300.15 and 75.47 MHz, respectively; chemical shifts are quoted in ppm relative to tetramethylsilane. ^{31}P{^{1}H}, ^{11}B{^{1}H}, and ^{7}Li{^{1}H} NMR spectra were recorded on a JEOL ECS500 spectrometer operating at 202.35, 160.16, and 194.38 MHz, respectively; chemical shifts are quoted in ppm relative to external 85% H_3PO_4, $BF_3{\cdot}Et_2O$, and 0.1 M LiCl, respectively. Signals due to BH$_3$ protons and the ^{1}H−^{31}P coupling constants for these signals were identified using selective ^{1}H{^{11}B} experiments. Elemental analyses were obtained by the Elemental Analysis Service of London Metropolitan University.

Preparation of $Ph_2P(BH_3)CH_2PiPr_2$ (1a). To a cold (0 °C) solution of $Ph_2P(BH_3)Me$ (2.16 g, 0.01 mol) in THF (30 mL) was added, dropwise, *n*BuLi (4.00 mL, 0.01 mol), and this solution was left to stir for 1 h while warming to room temperature. This solution was added to a cold (−78 °C) solution of *i*Pr$_2$PCl (1.6 mL, 0.01 mol) in THF (30 mL), and this mixture was stirred for 12 h, while warming slowly to room temperature. The solvent was removed *in vacuo* to give a pale yellow solid, which was extracted into dichloromethane (40 mL) and filtered; the solvent was removed *in vacuo* from the filtrate to give **1a** as a colorless solid, which was sufficiently clean for use without further purification. Yield: 2.67 g, 81%. ^{1}H{^{11}B} NMR ($CDCl_3$): 0.94 (dd, J_{HH} = 7.0, J_{PH} = 5.0 Hz, 6H, CH*Me*Me), 0.97 (dd, J_{HH} = 7.0, J_{PH} = 6.5 Hz, 6H, CHMe*Me*), 1.04 (d, J_{PH} = 16.3 Hz, 3H, BH$_3$), 1.73 (m, 2H, *CH*MeMe), 2.13 (dd, J_{PH} = 11.5, $J_{P'H}$ = 7.0 Hz, 2H, CH_2), 7.38−7.80 (m, 10H, ArH). ^{13}C{^{1}H} NMR ($CDCl_3$): δ 18.66 (dd, J_{PC} = 38.2, $J_{P'C}$ = 37.6 Hz, CH_2), 19.16 (d, J_{PC} = 13.6 Hz, CH*Me*Me), 19.22 (d,

dx.doi.org/10.1021/om5005995 | *Organometallics* XXXX, XXX, XXX−XXX

J_{PC} = 12.8 Hz, CHMe*Me*), 24.27 (dd, J_{PC} = 15.6, $J_{P'C}$ = 6.4 Hz, *CH*MeMe), 128.67 (d, J_{PC} = 9.8 Hz, Ar), 130.42 (dd, J_{PC} = 52.2, $J_{P'C}$ = 2.4 Hz, Ar), 131.21 (d, J_{PC} = 2.4 Hz, Ar), 132.72 (dd, J_{PC} = 9.1, $J_{P'C}$ = 9.1 Hz, Ar). $^{11}B\{^1H\}$ NMR ($CDCl_3$): δ −39.3 (d, J_{PB} = 49 Hz). $^{31}P\{^1H\}$ NMR ($CDCl_3$): δ −8.3 (d, J_{PP} = 73 Hz, P*i*Pr$_2$), 16.6 (br m, PPh$_2$).

Preparation of [Ph$_2$P(BH$_3$)CHP*i*Pr$_2$]Li(tmeda) (1b). To a cold (0 °C) solution of **1a** (0.42 g, 1.27 mmol) in THF (25 mL) was added *n*BuLi (0.51 mL, 1.27 mmol). This mixture was allowed to attain room temperature and was stirred for 1 h. One equivalent of tmeda (0.19 mL, 1.27 mmol) was added to the solution, and the resulting mixture was stirred for 10 min. Solvent was removed *in vacuo*, leaving a sticky orange solid, which was crystallized from cold (−30 °C) diethyl ether (10 mL) as yellow blocks. Yield: 0.53 g, 92%. Anal. Calcd for $C_{25}H_{44}BLiN_2P_2$ (452.34): C 66.38, H 9.80, N 6.19. Found: C 66.49, H 9.70, N 6.08. $^1H\{^{11}B\}$ NMR (d_8-toluene,): δ 1.06 (dd, J_{PH} = 15.5, J_{HH} = 7.0 Hz, 6H, CH*Me*Me), 1.12 (d, J_{PH} = 10.5 Hz, 3H, BH$_3$), 1.17 (dd, J_{PH} = 10.5, J_{HH} = 6.5 Hz, 6H, CHMe*Me*), 1.74 (m, 2H, *CH*MeMe), 1.76 (s, 4H, CH$_2$N), 1.93 (s, 12H, NMe$_2$), 7.06 (m, 2H, ArC), 7.18 (m, 4H, ArC), 8.06 (m, 4H, ArC). $^{13}C\{^1H\}$ NMR (d_8-toluene): δ 2.45 (dd, J_{PC} = 92.6, $J_{P'C}$ = 16.5 Hz, P$_2$CH), 18.47 (d, J_{PC} = 3.8 Hz, CH*Me*Me), 21.21 (d, J_{PC} = 15.0 Hz, CHMe*Me*), 25.86 (dd, J_{PC} = 8.3, $J_{P'C}$ = 4.2 Hz, *C*HMeMe), 46.29 (NMe$_2$), 56.93 (CH$_2$N), 127.54 (d, J_{PC} = 8.5 Hz, ArC), 131.84 (d, J_{PC} = 8.7 Hz, ArC), 143.86 (dd, J_{PC} = 57.4, $J_{P'C}$ = 5.5 Hz, *ipso*ArC) [remaining aromatic signal obscured by solvent]. $^7Li\{^1H\}$ NMR (d_8-toluene): δ 0.8 (d, J_{PLi} = 53 Hz). $^{11}B\{^1H\}$ NMR (d_8-toluene): δ −35.5 (d, J_{PB} = 94 Hz). $^{31}P\{^1H\}$ NMR (d_8-toluene): δ 9.1 (m, J_{PP} = 165, J_{PLi} = 53 Hz, P*i*Pr$_2$), 13.9 (m, J_{PP} = 165, J_{PB} = 94 Hz, PPh$_2$).

Preparation of [Ph$_2$P(BH$_3$)CHP*i*Pr$_2$]Li(THF)$_2$ (1c). To a cold (0 °C) solution of **1a** (0.82 g, 2.06 mmol) in THF (30 mL) was added *n*BuLi (0.68 mL, 2.06 mmol). This mixture was allowed to warm to room temperature and was stirred for 1 h. The solvent was removed *in vacuo*, leaving a sticky orange solid, which was crystallized from cold (−30 °C) diethyl ether (10 mL) as yellow-orange blocks. Yield: 0.47 g, 48%. Anal. Calcd for $C_{27}H_{44}BLiO_2P_2$ (480.34): C 67.51, H 9.23. Found: C 67.42, H 9.13. $^1H\{^{11}B\}$ NMR (d_8-toluene): δ 0.61 (br s, 3H, BH$_3$), 1.12 (dd, J_{PH} = 15.5, J_{HH} = 7.0 Hz, 6H, CH*Me*Me), 1.16 (dd, J_{PH} = 11.0, J_{HH} = 7.0 Hz, 6H, CHMe*Me*), 1.36 (m, 8H, THF), 1.79 (m, 2H, C*H*MeMe), 1.97 (dd, J_{PH} = 1.5, $J_{P'H}$ = 11.5 Hz, 1H, P$_2$CH), 3.50 (m, 8H, THF), 7.04 (m, 2H, ArH), 7.18 (m, 4H, ArH), 8.06 (m, 4H, ArH). $^{13}C\{^1H\}$ NMR (d_8-toluene): δ 2.74 (dd, J_{PC} = 93.4, $J_{P'C}$ = 14.3 Hz, P$_2$CH), 18.40 (d, J_{PC} = 3.8 Hz, CH*Me*Me), 20.88 (d, J_{PC} = 15.2 Hz, CHMe*Me*), 25.87 (dd, J_{PC} = 8.6, $J_{P'C}$ = 4.5 Hz, *C*HMeMe), 25.20 (THF), 68.15 (THF), 127.26 (d, J_{PC} = 9.4 Hz, ArC), 131.57 (d, J_{PC} = 8.7 Hz, ArC), 143.71 (dd, J_{PC} = 58.7, $J_{P'C}$ = 7.0 Hz, *ipso*-ArC) [remaining aromatic signal obscured by solvent]. $^7Li\{^1H\}$ NMR (d_8-toluene): δ 0.3 (s). $^{11}B\{^1H\}$ NMR (d_8-toluene): δ −36.1 (d, J_{PB} = 91 Hz). $^{31}P\{^1H\}$ NMR (d_8-toluene): δ 9.1 (d, J_{PP} = 166 Hz, P*i*Pr$_2$), 14.1 (m, J_{PB} = 91, J_{PP} = 166 Hz, P(BH$_3$)Ph$_2$).

Preparation of Ph$_2$PCH$_2$P(BH$_3$)*i*Pr$_2$ (2a). Compound **1a** (1.32 g, 4.07 mmol) was dissolved in toluene (30 mL), and this solution was heated under reflux for 12 h. The solvent was removed *in vacuo* to give **2a** as a viscous oil. Yield: 1.32 g, 100%. $^1H\{^{11}B\}$ NMR ($CDCl_3$): δ 0.37 (d, J_{PH} = 15.0 Hz, 3H, BH$_3$), 1.12 (dd, J_{PH} = 14.1, J_{HH} = 7.3 Hz, 6H, CH*Me*Me), 1.16 (dd, J_{PH} = 14.7, J_{HH} = 7.1 Hz, 6H, CHMe*Me*), 2.10 (m, 2H, C*H*MeMe), 2.37 (d, J_{PH} = 9.5 Hz, 2H, P$_2$CH$_2$), 7.33−7.51 (m, 10H, ArH). $^{13}C\{^1H\}$ NMR ($CDCl_3$): δ 17.25 (d, J_{PC} = 1.8 Hz, CH*Me*Me), 17.31 (d, J_{PC} = 2.8 Hz, CHMe*Me*), 19.87 (dd, J_{PC} = 33.0, $J_{P'C}$ = 26.7 Hz, CH$_2$), 22.58 (dd, J_{PC} = 32.2, $J_{P'C}$ = 4.0 Hz *C*HMeMe), 128.74 (d, J_{PC} = 7.3 Hz, ArC), 129.26 (ArC), 133.0 (d, J_{PC} = 20.7 Hz, ArC), 138.71 (dd, J_{PC} = 14.3, $J_{P'C}$ = 5.6 Hz, *ipso*-ArC). $^{11}B\{^1H\}$ NMR ($CDCl_3$): δ −43.5 (d, J_{PB} = 59 Hz). $^{31}P\{^1H\}$ NMR ($CDCl_3$): δ −26.7 (d, J_{PP} = 38 Hz, PPh$_2$), 35.5 (m, P(BH$_3$)*i*Pr$_2$).

Preparation of [Ph$_2$PCH{P(BH$_3$)*i*Pr$_2$}]Li(tmeda) (2b). To a cold (0 °C) solution of **1b** (1.24 g, 3.76 mmol) in THF (30 mL) was added *n*BuLi (1.50 mL, 3.76 mmol). This mixture was allowed to warm to room temperature and was stirred for 1 h. To this solution was added tmeda (0.57 mL, 3.76 mmol), and this mixture was stirred for 5 min. Solvent was removed *in vacuo*, leaving an orange oil, which was crystallized from cold (−30 °C) hexamethyldisiloxane (10 mL) to give **2b** as a pale yellow, crystalline solid. Yield: 0.59 g, 35%. Anal. Calcd for $C_{25}H_{44}BLiN_2P_2$ (452.34): C 66.38, H 9.80, N 6.19. Found: C 66.47, H 9.70, N 6.04. ^1H NMR (d_6-benzene): δ 0.87 (dd, J_{PH} = 11.0, $J_{P'H}$ = 3.0 Hz, 1H, P$_2$CH), 1.29 (dd, J_{PH} = 14.5, J_{HH} = 7.5 Hz, 6H, CH*Me*Me), 1.31 (t, $J_{PH/HH}$ = 7.6 Hz, 6H, CHMe*Me*), 1.99 (m, 2H, C*H*MeMe), 7.10 (m, 2H, ArH), 7.25 (m, 4H, ArH), 7.83 (m, 4H, ArH). $^{13}C\{^1H\}$ NMR (d_6-benzene): δ 3.08 (dd, J_{PC} = 84.3, $J_{P'C}$ = 23.9 Hz, P$_2$CH), 17.04 (d, J_{PC} = 1.7 Hz, CH*Me*Me), 18.05 (CHMe*Me*), 25.73 (dd, J_{PC} = 40.9, $J_{P'C}$ = 5.3 Hz, *C*HMeMe), 45.80 (NMe$_2$), 56.42 (CH$_2$N), 126.48 (ArC), 127.70 (d, J_{PC} = 6.7 Hz, ArC), 131.94, 132.07 (ArC), 148.79 (dd, J_{PC} = 7.7, $J_{P'C}$ = 4.9 Hz, *ipso*-ArC). $^7Li\{^1H\}$ NMR (d_6-benzene): δ 0.9 (d, J_{PLi} = 62 Hz). $^{11}B\{^1H\}$ NMR (d_6-benzene): δ −41.1 (d, J_{PB} = 95 Hz). $^{31}P\{^1H\}$ NMR (d_6-benzene): δ −6.7 (m, J_{PP} = 165, J_{PLi} = 62 Hz, PPh$_2$), 32.2 (m, J_{PP} = 165, J_{PB} = 95 Hz, P*i*Pr$_2$).

Preparation of Ph$_2$P(BH$_3$)CH$_2$P(BH$_3$)*i*Pr$_2$ (3a). To a solution of **1a** (0.51 g, 1.54 mmol) in THF (25 mL) was added BH$_3$·SMe$_2$ (0.77 mL, 1.54 mmol), and this solution was stirred for 1 h. The solvent was removed *in vacuo* to give **3a** as a white solid. Yield: 0.49 g, 92%. $^1H\{^{11}B\}$ NMR ($CDCl_3$): δ 0.22 (d, J_{PH} = 14.8 Hz, 3H, BH$_3$), 1.08 (dd, J_{PH} = 15.1, J_{HH} = 6.9 Hz, 6H, CH*Me*Me), 1.15 (dd, J_{PH} = 15.1, J_{HH} = 6.9 Hz, 6H, CHMe*Me*), 1.17 (d, J_{PH} = 15.1 Hz, 3H, BH$_3$), 2.42 (m, 2H, C*H*MeMe), 2.59 (dd, J_{PH} = 11.8, $J_{P'H}$ = 10.2 Hz, 2H, P$_2$CH$_2$), 7.44−7.76 (m, 10H, ArH). $^{13}C\{^1H\}$ NMR ($CDCl_3$): δ 17.58 (CH*Me*Me), 17.96 (CHMe*Me*), 18.54 (dd, J_{PC} = 23.9, $J_{P'C}$ = 18.9 Hz, *C*HMeMe), 129.04 (d, J_{PC} = 10.1 Hz, ArC), 129.94 (dd, J_{PC} = 56.6, $J_{P'C}$ = 2.5 Hz, *ipso*ArC), 131.78 (d, J_{PC} = 2.5 Hz, ArC), 132.29 (d, J_{PC} = 10.1 Hz, ArC). $^{11}B\{^1H\}$ NMR ($CDCl_3$): δ −43.3 (d, J_{PB} = 42 Hz), −39.0 (d, J_{PB} = 56 Hz). $^{31}P\{^1H\}$ NMR ($CDCl_3$): δ 12.6 (br m), 40.8 (br m).

Preparation of [{Ph$_2$P(BH$_3$)}CH{P(BH$_3$)*i*Pr$_2$}]Li(tmeda) (3b). To a cold (0 °C) solution of **3a** (0.50 g, 1.48 mmol) in THF (25 mL) was added *n*BuLi (0.59 mL, 1.48 mmol), and this solution was stirred for 1 h while warming to room temperature. To the resulting solution was added tmeda (0.22 mL, 1.48 mmol), and this mixture was stirred for 10 min. The solvent was removed *in vacuo* to leave a yellow oil, which was crystallized from cold (5 °C) diethyl ether (10 mL) to give **3b** as a pale yellow, crystalline solid. Yield: 0.31 g, 45%. Anal. Calcd for $C_{25}H_{47}B_2LiN_2P_2$ (466.17): C 64.41, H 10.16, N 6.01. Found: C 64.29, H 10.01, N 5.85. $^1H\{^{11}B\}$ NMR (d_8-toluene): δ 0.33 (dd, J_{PH} = 10.5, $J_{P'H}$ = 12.6 Hz, 1H, P$_2$CH), 0.53 (d, J_{PH} = 15.2 Hz, 3H, BH$_3$), 1.17 (d, J_{PH} = 17.0 Hz, 3H, BH$_3$), 1.23 (dd, J_{PH} = 7.0, J_{HH} = 6.8 Hz, 6H, CH*Me*Me), 1.24 (dd, J_{PH} = 6.9, J_{HH} = 5.3 Hz, 6H, CHMe*Me*), 1.74 (s, 4H, CH$_2$N), 1.83 (m, 2H, C*H*MeMe), 1.97 (s, 12H, NMe$_2$), 7.07 (m, 2H, ArH), 7.18 (m, 4H, ArH), 8.02 (m, 4H, ArH). $^{13}C\{^1H\}$ NMR (d_8-toluene): δ −1.52 (dd, J_{PC} = 90.6, $J_{P'C}$ = 78.1 Hz, P$_2$CH), 16.58 (d, J_{PC} = 1.9 Hz, CH*Me*Me), 17.44 (d, J_{PC} = 0.6 Hz, CHMe*Me*), 26.56 (dd, J_{PC} = 41.8, $J_{P'C}$ = 4.4 Hz, *C*HMeMe), 45.64 (NMe$_2$), 56.74 (CH$_2$N), 127.39 (d, J_{PC} = 9.6 Hz, ArC), 128.00 (d, J_{PC} = 2.4 Hz, ArC), 131.57 (d, J_{PC} = 9.1 Hz, ArC), 143.34 (dd, J_{PC} = 61.0, $J_{P'C}$ = 4.4 Hz, *ipso*ArC). $^7Li\{^1H\}$ NMR (d_8-toluene): δ 0.6 (s). $^{11}B\{^1H\}$ NMR (d_8-toluene): δ −40.9 (d, J_{PB} = 92 Hz), −35.7 (d, J_{PB} = 88 Hz). $^{31}P\{^1H\}$ NMR (d_8-toluene): δ 11.4 (br m), 26.6 (br m).

Preparation of Ph$_2$PCH$_2$P*i*Pr$_2$ (4a). A solution of **1a** (1.04 g, 3.15 mmol) in degassed methanol (50 mL) was heated under reflux for 24 h. The solution was cooled to room temperature, and volatiles were removed *in vacuo* to leave **4a** as a colorless oil. Yield: 0.88 g, 88%. ^1H NMR ($CDCl_3$): δ 1.04 (m, 6H, CHMe*Me*), 1.09 (m, 6H, CH*Me*Me), 1.83 (m, 2H, C*H*MeMe), 2.06 (br, 2H, CH$_2$P$_2$), 7.31−7.35 (m, 6H, ArH), 7.45−7.49 (m, 4H, ArH). $^{13}C\{^1H\}$ NMR ($CDCl_3$): δ 19.00 (d, J_{PC} = 10.1 Hz, CHMe*Me*), 19.77 (d, J_{PC} = 14.9 Hz, CH*Me*Me), 20.87 (m, CH$_2$P$_2$), 24.34 (m, CHMeMe), 128.44 (d, J_{PC} = 6.5 Hz, Ar), 128.68, 133.01 (Ar), 139.62 (br, *ipso*-Ar). $^{31}P\{^1H\}$ NMR ($CDCl_3$): δ −19.2 (d, J_{PP} = 123 Hz, PPh$_2$), −3.8 (d, J_{PP} = 123 Hz, P*i*Pr$_2$).

Preparation of [Ph$_2$PCHP*i*Pr$_2$]Li(tmeda) (4b). To a solution of **4a** (0.54 g, 1.71 mmol) in THF (10 mL) was added *n*BuLi (0.7 mL, 1.75 mmol) and tmeda (0.2 mL, 0.26 g, 2.24 mmol), and this solution was stirred for 1 h. Solvent was removed *in vacuo*, the sticky yellow residue was dissolved in diethyl ether (5 mL), and this solution was cooled to 5 °C for 16 h. The pale yellow crystals of **4b** were isolated

dx.doi.org/10.1021/om5005995 | *Organometallics* XXXX, XXX, XXX−XXX

and washed with a little light petroleum. Yield: 0.65 g, 87%. Anal. Calcd for $C_{25}H_{41}LiN_2P_2$ (438.50): C 68.48, H 9.42, N 6.39. Found: C 68.37, H 9.29, N 6.28. ^{1}H NMR (d_8-THF): 0.93 (dd, J_{PH} = 14.6, J_{HH} = 6.7 Hz, 6H, CHMe*Me*), 0.95 (m, 1H, CHLi), 1.00 (dd, J_{PH} = 10.7, J_{HH} = 7.0 Hz, 6H, CH*Me*Me), 1.52 (m, 2H, C*H*MeMe), 2.14 (s, 12H, NMe_2), 2.29 (s, 4H, CH_2N), 6.89 (m, 2H, ArH), 7.02 (m, 4H, ArH), 7.52 (m, 4H, ArH). ^{13}C{^{1}H} NMR (d_8-THF): δ 9.52 (m, CHLi), 18.42 (d, J_{PC} = 4.4 Hz, CHMe*Me*), 20.90 (d, J_{PC} = 16.7 Hz, CH*Me*Me), 26.51 (d, J_{PC} = 14.7 Hz, *C*HMeMe), 45.35 (NMe_2), 57.93 (CH_2N), 124.30 (Ar), 126.33 (d, J_{PC} = 5.6 Hz, Ar), 130.92 (d, J_{PC} = 15.2 Hz, Ar), 152.24 (dd, J_{PC} = 15.1, $J_{P'C}$ = 10.4 Hz, Ar). ^{7}Li NMR (d_8-THF): δ 0.1 (s). ^{31}P{^{1}H} NMR: δ 0.4 (d, J_{PP} = 381 Hz, PPh_2), 20.9 (d, J_{PP} = 381 Hz, P*i*Pr$_2$).

Kinetic Studies. The kinetic studies on the isomerization of **1a** to **2a** were carried out on 0.17 M solutions in toluene (taken from a stock solution kept at −30 °C). ^{31}P{^{1}H} NMR spectra were recorded over 5 min at 20 min intervals with a repetition time of 3 s. The spin−lattice relaxation times of the ^{31}P nuclei of **1a** and **2a** were determined to be nearly identical (T_1 = 5.79 and 5.86 s, respectively), and so integrals were measured directly from the spectra with no correction.

Crystal Structure Determinations of 1a, 1b, 1c, 2b, 3b, and 4b. Measurements were made at 150 K on an Oxford Diffraction (Agilent Technologies) Gemini A Ultra diffractometer, using Cu Kα radiation (λ = 1.541 78 Å; **1a**) or Mo Kα radiation (λ = 0.710 73 Å; **1b**−**4b**, **1c**). Cell parameters were refined from the observed positions of all strong reflections. Intensities were corrected semiempirically for absorption, based on symmetry-equivalent and repeated reflections. The structures were solved by direct methods and refined on F^2 values for all unique data (see the Supporting Information for further details). All non-hydrogen atoms were refined anisotropically, and C-bound H atoms were constrained with a riding model, while B-bound H atoms were freely refined; U(H) was set at 1.2 (1.5 for methyl groups) times U_{eq} for the parent C atom. Programs were Oxford Diffraction CrysAlisPro for data collection and processing and SHELXTL for structure solution, refinement, and molecular graphics.[26]

DFT Calculations. Geometry optimizations were performed with the Gaussian09 suite of programs (revision B.01, C.01, or D.01).[27] Ground-state optimizations were performed using the GGA meta-hybrid wB97XD functional,[13] which includes a correction for dispersion effects; the 6-311+G(d,p) all-electron basis set[16] was used on all atoms [default parameters were used throughout]. The global minimum energy conformations of **1a′**−**4a′** were located by relaxed potential energy surface scans at the HF/3-21G* level in which the P−C−P−C(*i*Pr) dihedral angle was increased in 10° steps through a full 360° rotation; the located minimum energy geometries were then reoptimized at the wB97XD/6-311+G(d,p) level. The identity of minima was confirmed by the absence of imaginary vibrational frequencies in each case. Natural bond orbital analyses were performed using the NBO 3.1 module of Gaussian09.[23] For the rearrangement of **1a′** to **2a′** the transition states $\mathbf{1}_{intra}$′ and $\mathbf{1}_{inter}$′ were initially located using the QST3 method[28] at the HF/3-21G* level;[29] the geometries obtained were then reoptimized at the wB97XD/6-311+G(d,p) level. The nature of these transition states was confirmed by the presence of a single imaginary vibrational frequency, which correlated with the expected displacement vector for migration of the BH_3 group between the two phosphine centers in each case. For the dissociation of **1a′** and **3a′** and the migration of BH_3 between two molecules of **1a′** via $\mathbf{1}_{inter}$′ the free energy was corrected for basis set superposition error (using the counterpoise method);[30] the absence of a transition state for the dissociation of both **1a′** and **3a′** was confirmed by performing a relaxed potential energy surface scan, increasing the P−B distance in 20 increments of 0.1 Å, which showed no maximum on the pathway to complete dissociation. In all calculations solvation by toluene was included implicitly using the IEF Polarizable Continuum Model.[17] All energies were corrected to 298.15 K.

■ ASSOCIATED CONTENT

Ⓢ Supporting Information

For **1a**−**4a** ^{1}H, ^{13}C{^{1}H}, ^{11}B{^{1}H} and ^{31}P{^{1}H} NMR spectra. For **1a**, **1b**, **1c**, **2b**, **3b**, and **4b** details of structure determination, atomic coordinates, bond lengths and angles, and displacement parameters in CIF format; details of the molecular structures of **1a** and **1c**. For the conversion of **1** into **2a** a plot showing the concentration dependence of the reaction and an Eyring plot from whence the thermodynamic parameters were derived. For **1a′**−**4a′**, **1b′**−**4b′**, $\mathbf{1}_{intra}$′, and $\mathbf{1}_{inter}$′ details of DFT calculations, final atomic coordinates, and energies. The supplemental file combined.xyz contains the computed Cartesian coordinates of all of the molecules reported in this study. The file may be opened as a text file to read the coordinates or opened directly by a molecular modeling program such as Mercury (version 3.3 or later, http://www.ccdc.cam.ac.uk/pages/Home.aspx) for visualization and analysis. This material is available free of charge via the Internet at http://pubs.acs.org.

■ AUTHOR INFORMATION

Corresponding Authors

*E-mail: keith.izod@ncl.ac.uk.

*E-mail: corinne.wills@ncl.ac.uk.

Notes

The authors declare no competing financial interest.

■ ACKNOWLEDGMENTS

The authors are grateful to Newcastle University for financial support and to Prof. R. A. Henderson (Newcastle) for helpful discussions of the kinetic data and would like to acknowledge the use of the EPSRC UK National Service for Computational Chemistry Software (NSCCS) at Imperial College London in carrying out this work.

■ REFERENCES

(1) For recent reviews on the chemistry of phosphine-borane adducts and their applications see: (a) Ohff, M.; Holz, J.; Quirmbach, M.; Borner, A. *Synthesis* **1998**, 1391. (b) Brunel, J. M.; Faure, B.; Maffei, M. *Coord. Chem. Rev.* **1998**, *178*−*180*, 665. (c) Carboni, B.; Monnier, L. *Tetrahedron* **1999**, *55*, 1197. (d) Gaumont, A. C.; Carboni, B. In *Science of Synthesis*; Kaufmann, D.; Matteson, D. S., Eds.; Thieme: Stuttgart, 2004; Vol. *6*, pp 485−512. (e) Staubitz, A.; Robertson, A. P. M.; Sloan, M. E.; Manners, I. *Chem. Rev.* **2010**, *110*, 4023.

(2) (a) Imamoto, T.; Oshiki, T.; Onazawa, T.; Kusumoto, T.; Sato, K. *J. Am. Chem. Soc.* **1990**, *112*, 5244. (b) Wolfe, B.; Livinghouse, T. *J. Am. Chem. Soc.* **1998**, *120*, 5116. (c) Brisset, H.; Gourdel, Y.; Pellon, P.; Le Corre, M. *Tetrahedron Lett.* **1993**, *34*, 4523. (d) Desponds, O.; Huynh, C.; Schlosser, M. *Synthesis* **1998**, 983.

(3) (a) van Overschelde, M.; Vervecken, E.; Modha, S. G.; Cogen, S.; van der Eycken, E.; van der Eycken, J. *Tetrahedron* **2009**, *65*, 6410. (b) Schröder, M.; Nozaki, K.; Hiyama, T. *Bull. Chem. Soc. Jpn.* **2004**, *77*, 1931.

(4) (a) McKinstry, L.; Livinghouse, T. *Tetrahedron* **1995**, *51*, 7655. (b) McKinstry, L.; Livinghouse, T. *Tetrahedron Lett.* **1994**, *35*, 9319.

(5) For s-block metal complexes see: (a) Izod, K.; McFarlane, W.; Tyson, B. V.; Clegg, W.; Harrington, R. W. *Chem. Commun.* **2004**, 570. (b) Izod, K.; Wills, C.; Clegg, W.; Harrington, R. W. *Organometallics* **2006**, *25*, 38. (c) Izod, K.; Wills, C.; Clegg, W.; Harrington, R. W. *Organometallics* **2006**, *25*, 5326. (d) Izod, K.; Wills, C.; Clegg, W.; Harrington, R. W. *Inorg. Chem.* **2007**, *46*, 4320. (e) Izod, K.; Wills, C.; Clegg, W.; Harrington, R. W. *Organometallics* **2007**, *26*, 2861. (f) Izod, K.; Wills, C.; Clegg, W.; Harrington, R. W. *Dalton Trans.* **2007**, 3669. (g) Izod, K.; Wills, C.; Clegg, W.; Harrington, R. W. *J. Organomet. Chem.* **2007**, *692*, 5060. (h) Izod, K.; Bowman, L. J.; Wills, C.; Clegg,

W.; Harrington, R. W. *Dalton Trans.* **2009**, 3340. (i) Izod, K.; Wills, C.; Clegg, W.; Harrington, R. W. *Organometallics* **2010**, *29*, 4774. (j) Langer, J.; Wimmer, K.; Görls, H.; Westerhausen, M. *Dalton Trans.* **2009**, 2951. (k) Orzechowski, L.; Jansen, G.; Lutz, M.; Harder, S. *Dalton Trans.* **2009**, 2958. (l) Sun, X.-M.; Manabe, K.; Lam, W. W.-L.; Shiraishi, N.; Kobayashi, J.; Shiro, M.; Utsumi, H.; Kobayashi, S. *Chem.—Eur. J.* **2005**, *11*, 361. (m) Schmidbaur, H.; Weiss, E.; Zimmer-Gasse, B. *Angew. Chem., Int. Ed. Engl.* **1979**, *18*, 782.

(6) For recent examples of d- and f-block metal complex see: (a) Blug, M.; Grünstein, D.; Alcaraz, G.; Sabo-Etienne, S.; Le Goff, X.-F.; Le Floch, P.; Mézailles, N. *Chem. Commun.* **2009**, 4432. (b) Izod, K.; Clegg, W.; Harrington, R. W. *Dalton Trans.* **2010**, *39*, 6705.

(7) For p-block metal complexes see: (a) Izod, K.; McFarlane, W.; Tyson, B. V.; Carr, I.; Clegg, W.; Harrington, R. W. *Organometallics* **2006**, *25*, 1135. (b) Izod, K.; McFarlane, W.; Wills, C.; Clegg, W.; Harrington, R. W. *Organometallics* **2008**, *27*, 4386. (c) Izod, K.; Wills, C.; Clegg, W.; Harrington, R. W. *Organometallics* **2009**, *28*, 2211. (d) Izod, K.; Wills, C.; Clegg, W.; Harrington, R. W. *Organometallics* **2009**, *28*, 5661. (e) Wills, C.; Izod, K.; Clegg, W.; Harrington, R. W. *Dalton Trans.* **2010**, *39*, 2379. (f) Izod, K.; Wills, C.; Harrington, R. W.; Clegg, W. *J. Organomet. Chem.* **2013**, *725*, 11.

(8) (a) Alford, K. J.; Bishop, E. O.; Carey, P. R.; Smith, J. D. *J. Chem. Soc. (A)* **1971**, 2574. (b) Alaluf, E.; Alford, K. J.; Bishop, E. O.; Smith, J. D. *J. Chem. Soc., Dalton Trans.* **1974**, 669. (c) Alford, K. J.; Bishop, E. O.; Smith, J. D. *J. Chem. Soc., Dalton Trans.* **1976**, 920.

(9) Verdenne, P.; Le Guen, V.; Toupet, L.; Le Gall, T.; Mioskowski, C. *J. Am. Chem. Soc.* **1999**, *121*, 1090.

(10) DiMare, M. *J. Org. Chem.* **1996**, *61*, 8378.

(11) For selected references on the mechanism of exchange of amine-borane adducts see: (a) Budde, W. L.; Hawthorne, M. F. *J. Am. Chem. Soc.* **1971**, *93*, 3147. (b) Walmsley, D. E.; Budde, W. L.; Hawthorne, M. F. *J. Am. Chem. Soc.* **1971**, *93*, 3150. (c) Lalor, F. J.; Paxson, T.; Hawthorne, M. F. *J. Am. Chem. Soc.* **1971**, *93*, 3156. (d) Cowley, A. H.; Mills, J. L. *J. Am. Chem. Soc.* **1969**, *91*, 2911. (e) Toyota, S.; Futuwaka, T.; Ikeda, H.; Oki, M. *J. Chem. Soc., Chem. Commun.* **1995**, 2499.

(12) Loschen, C.; Voigt, K.; Frunzke, J.; Deifenbach, A.; Diedenhofen, M.; Frenking, G. *Z. Anorg. Allg. Chem.* **2002**, *628*, 1294.

(13) Chai, J.-D.; Head-Gordon, M. *Phys. Chem. Chem. Phys.* **2008**, *10*, 6615.

(14) Zhao, Y.; Truhlar, D. G. *Theor. Chem. Acc.* **2008**, *120*, 215.

(15) (a) Becke, A. D. *J. Chem. Phys.* **1993**, *98*, 5648. (b) Stephens, P. J.; Devlin, F. J.; Chablowski, C. F.; Frisch, M. J. *J. Phys. Chem.* **1994**, *98*, 11623. (c) Hertwig, R. H.; Koch, W. *Chem. Phys. Lett.* **1997**, *268*, 345.

(16) (a) McLean, A. D.; Chandler, G. S. *J. Chem. Phys.* **1980**, *72*, 5639. (b) Raghavachari, K.; Binkley, J. S.; Seeger, R.; Pople, J. A. *J. Chem. Phys.* **1980**, *72*, 650. (c) Binning, R. C., Jr.; Curtiss, L. A. *J. Comput. Chem.* **1990**, *11*, 1206. (d) McGrath, M. P.; Radom, L. *J. Chem. Phys.* **1991**, *94*, 511. (e) Curtiss, L. A.; McGrath, M. P.; Blaudeau, J.-P.; Davis, N. E.; Binning, R. C., Jr.; Radom, L. *J. Chem. Phys.* **1995**, *103*, 6104.

(17) Tomasi, J.; Mennucci, B.; Cammi, R. *Chem. Rev.* **2005**, *105*, 2999.

(18) Langer, J.; Pálfi, V. K.; Görls, H.; Reiher, M.; Westerhausen, M. *Chem. Commun.* **2013**, *49*, 1121.

(19) (a) Izod, K. *Coord. Chem. Rev.* **2002**, *227*, 153. (b) Izod, K. *Adv. Inorg. Chem.* **2000**, *50*, 33.

(20) (a) Karsch, H. H.; Richter, R.; Paul, M.; Riede, J. *J. Organomet. Chem.* **1994**, *474*, C1. (b) Karsch, H. H.; Richter, R.; Deubelly, B.; Schier, A.; Paul, M.; Heckel, M.; Angermeier, K.; Hiller, W. *Z. Naturforsch. B* **1994**, *49b*, 1798.

(21) Müller, G.; Brand, J. *Organometallics* **2003**, *22*, 1463.

(22) (a) Giese, H.-H.; Habereder, T.; Nöth, H.; Ponikwar, W.; Thomas, S.; Warchhold, M. *Inorg. Chem.* **1999**, *38*, 4188. (b) Armstrong, D. R.; Clegg, W.; Colquhoun, H. M.; Daniels, J. A.; Mulvey, R. E.; Stephenson, I. R.; Wade, K. *J. Chem. Soc., Chem. Commun.* **1987**, 630.

(23) (a) *NBO 3.1*, Glendening, E. D.; Reed, A. E.; Carpenter, J. E.; Weinhold, F.; Theoretical Chemistry Institute, University of Wisconsin, Madison, 1996. (b) Carpenter, J. E.; Weinhold, F. *J. Mol. Struct. (THEOCHEM)* **1988**, *169*, 41. (c) Carpenter, J. E., Ph.D. thesis, University of Wisconsin, Madison, WI, 1987. (d) Foster, J. P.; Weinhold, F. *J. Am. Chem. Soc.* **1980**, *102*, 7211. (e) Reed, A. E.; Weinhold, F. *J. Chem. Phys.* **1983**, *78*, 4066. (f) Reed, A. E.; Weinhold, F. *J. Chem. Phys.* **1983**, 1736. (g) Reed, A. E.; Weinstock, R. B.; Weinhold, F. *J. Chem. Phys.* **1985**, *83*, 735. (h) Reed, A. E.; Curtiss, L. A.; Weinhold, F. *Chem. Rev.* **1988**, *88*, 899.

(24) Heuclin, H.; Fustier-Boutignon, M.; Ho, S. Y.-F.; Le Goff, X.-F.; Carenco, S.; So, C.-W.; Mézailles, N. *Organometallics* **2013**, *32*, 498.

(25) Riegel, N.; Darcel, C.; Stéphan, O.; Jugé, S. *J. Organomet. Chem.* **1998**, *567*, 219.

(26) (a) *CrysAlisPro*; Oxford Diffraction Ltd, Oxford, UK, 2008. (b) Sheldrick, G. M. *Acta Crystallogr., Sect. A* **2008**, *64*, 112.

(27) Frisch, M. J.; Trucks, G. W.; Schlegel, H. B.; Scuseria, G. E.; Robb, M. A.; Cheeseman, J. R.; Scalmani, G.; Barone, V.; Mennucci, B.; Petersson, G. A.; Nakatsuji, H.; Caricato, M.; Li, X.; Hratchian, H. P.; Izmaylov, A. F.; Bloino, J.; Zheng, G.; Sonnenberg, J. L.; Hada, M.; Ehara, M.; Toyota, K.; Fukuda, R.; Hasegawa, J.; Ishida, M.; Nakajima, T.; Honda, Y.; Kitao, O.; Nakai, H.; Vreven, T.; Montgomery, J. A., Jr.; Peralta, J. E.; Ogliaro, F.; Bearpark, M.; Heyd, J. J.; Brothers, E.; Kudin, K. N.; Staroverov, V. N.; Kobayashi, R.; Normand, J.; Raghavachari, K.; Rendell, A.; Burant, J. C.; Iyengar, S. S.; Tomasi, J.; Cossi, M.; Rega, N.; Millam, N. J.; Klene, M.; Knox, J. E.; Cross, J. B.; Bakken, V.; Adamo, C.; Jaramillo, J.; Gomperts, R.; Stratmann, R. E.; Yazyev, O.; Austin, A. J.; Cammi, R.; Pomelli, C.; Ochterski, J. W.; Martin, R. L.; Morokuma, K.; Zakrzewski, V. G.; Voth, G. A.; Salvador, P.; Dannenberg, J. J.; Dapprich, S.; Daniels, A. D.; Farkas, Ö.; Foresman, J. B.; Ortiz, J. V.; Cioslowski, J.; Fox, D. J. *Gaussian 09*, Revisions B.01, C.01, and D.01; Gaussian, Inc.: Wallingford, CT, 2009.

(28) (a) Peng, C.; Schlegel, H. B. *Isr. J. Chem.* **1993**, *33*, 449. (b) Peng, C.; Ayala, P. Y.; Schlegel, H. B.; Frisch, M. J. *J. Comput. Chem.* **1996**, *17*, 49. (c) Ayala, P. Y.; Schlegel, H. B. *J. Chem. Phys.* **1997**, *107*, 375.

(29) (a) Binkley, J. S.; Pople, J. A.; Hehre, W. J. *J. Am. Chem. Soc.* **1980**, *102*, 939. (b) Gordon, M. S.; Binkley, J. S.; Pople, J. A.; Pietro, W. J.; Hehre, W. J. *J. Am. Chem. Soc.* **1982**, *104*, 2797. (c) Pietro, W. J.; Francl, M. M.; Hehre, W. J.; Defrees, D. J.; Pople, J. A.; Binkley, J. S. *J. Am. Chem. Soc.* **1982**, *104*, 5039. (d) Dobbs, K. D.; Hehre, W. J. *J. Comput. Chem.* **1986**, *7*, 359. (e) Dobbs, K. D.; Hehre, W. J. *J. Comput. Chem.* **1987**, *8*, 861. (f) Dobbs, K. D.; Hehre, W. J. *J. Comput. Chem.* **1987**, *8*, 880.

(30) (a) Simon, S.; Duran, M.; Dannenberg, J. J. *J. Chem. Phys.* **1996**, *105*, 11024. (b) Boys, S. F.; Bernardi, F. *Mol. Phys.* **1970**, *19*, 553.